

1 TITLE: Anatomically-specific coupling between innate immune gene repertoire and  
2 microbiome structure during coral evolution

3 SHORT TITLE: Coral innate immunity and the microbiome

4 CLASSIFICATION: Biological Sciences

5 MINOR CATEGORY: Microbiology

6 AUTHORS:

7 Tanya Brown<sup>1</sup>

8 Dylan Sonett<sup>2</sup>

9 Ryan McMinds<sup>3</sup>

10 F. Joseph Pollock<sup>4</sup>

11 Mónica Medina<sup>5</sup>

12 Jesse R. Zaneveld<sup>1</sup> #

13 AFFILIATIONS:

14 <sup>1</sup> University of Washington, Bothell, School of Science, Technology, Engineering, and  
15 Mathematics, Division of Biological Sciences, UWBB-277, Bothell, WA 98011,  
16 USA

17 <sup>2</sup> School of Pharmacy, University of Washington, Seattle, Washington, USA

18 <sup>3</sup> Center for Global Health and Infectious Diseases Research, University of South  
19 Florida, 13201 Bruce B. Downs Blvd, MDC 56, Tampa, FL 33612, USA

20 <sup>4</sup> Hawai'i & Palmyra Program, The Nature Conservancy, Honolulu, HI, USA, 96817

21 <sup>5</sup> Pennsylvania State University, Department of Biology, 208 Mueller Lab, University  
22 Park, PA 16802, USA

23 # Corresponding author

24 CORRESPONDENCE TO: Jesse Robert Zaneveld

25 University of Washington, Bothell, Department of Biology, UWBB-277, Bothell, WA  
26 98011, USA

27 Telephone: 541-760-2411; Fax: 541-737-0496

28 Email: zaneveld@gmail.com

29 KEYWORDS: coral, microbiome, coevolution

30 ***Abstract***

31

32 Tropical reef-building corals exist in intimate symbiosis with diverse microbes and  
33 viruses. Coral microbiomes are generally much less diverse than their environment, but  
34 across studied corals, the biodiversity of these microbiomes varies greatly. It has  
35 previously been hypothesized that differences in coral innate immunity in general, and

36 the copy number of TIR-domain containing innate immune genes in particular, may drive  
37 interspecific differences in microbiome structure. Despite many existing studies of coral  
38 microbiomes, this hypothesis has previously been difficult to test due to a lack of  
39 consistently collected cross-species data on coral microbiomes. In this manuscript, we  
40 reannotate TIR-domain containing genes across diverse coral genomes, and use  
41 phylogenetic comparative methods to compare these innate immune gene copy numbers  
42 against 16S rRNA marker gene data on coral mucus, tissue, and skeleton microbiomes  
43 from the Global Coral Microbiome Project (GCMP). The copy number of Toll-like  
44 receptor (TLRs) and Interleukin-1 receptor (IL-1Rs) gene families, as well as the total  
45 genomic count of their constituent domains (LRR and TIR domains; and Ig and TIR  
46 domains, respectively), explained most interspecific differences in microbiome richness  
47 and beta-diversity among corals with sequenced genomes. We find that these correlations  
48 are also anatomically specific, with an especially strong correlation between IL-1R gene  
49 copy numbers and microbiome richness in the coral's endolithic skeleton. Together, these  
50 results suggest innate immunity may play a key role in sculpting microbiome structure in  
51 corals.

52

### 53 ***Introduction***

54

55 The 1681 described species of scleractinian corals<sup>1</sup> are environmentally critical  
56 ecosystem engineers that underpin many tropical reef ecosystems. Microbiomes are  
57 important contributors to the health of these tropical corals, with competing and  
58 cooperating microbes influencing animal health<sup>2</sup>. Therefore, evaluating how corals  
59 regulate this microbiome is of great importance. Numerous studies have uncovered  
60 important features of coral microbiomes, including the relative influence of differences  
61 across host anatomy<sup>3,4</sup>, between species<sup>4,5</sup>, among reefs<sup>6-8</sup>, and along environmental  
62 gradients<sup>8,9</sup>. This literature has also extensively documented coral microbiome responses  
63 to various stressors, including heat<sup>10,11</sup>, bleaching<sup>12,13</sup>, sedimentation<sup>14,15</sup>, nutrient  
64 pollution<sup>10,14,16</sup>, predation<sup>16</sup>, plastic pollution<sup>17</sup>, turf or macro-algal competition<sup>16,18,19</sup>,  
65 etc. Genetic studies within coral species have further found genotypic differences that  
66 correlate with microbiome composition<sup>20,21</sup>. Building on these ecological and population-  
67 genetic comparisons, specific coral microorganisms have been linked to important host  
68 health outcomes, such as protection against pathogens or susceptibility to them<sup>22</sup>. Recent  
69 microbiome manipulation experiments have even begun to establish the causal role of  
70 specific coral-associated bacteria in influencing key host traits like heat resistance<sup>23</sup>.  
71 Despite this thriving literature on coral microbiomes, the broader scale patterns of how  
72 modern coral microbiomes have evolved, and which host traits, if any, drive the large  
73 differences in microbiome structure and function seen between modern corals is not yet  
74 clear.

75

76 Increased attention to the question of how host traits have sculpted coral microbiomes  
77 over evolution is important. Comparative studies of coral microbiome evolution may  
78 identify host traits that have regulated coral microbiomes up to the present day.  
79 Comparative studies of coral microbiome evolution will also clarify a key part of the  
80 broader story of animal microbiome evolution. While vertebrate gut microbiomes are

81 structured by both host phylogenetic relatedness and convergently evolved host traits like  
82 diet or flight<sup>24,25</sup>, the traits shaping the microbiome evolution of basally divergent animal  
83 taxa are less clear.

84  
85 Among the many coral traits that could influence microbiome structure, differences in  
86 innate immunity are promising candidates, since they have the potential to directly  
87 regulate the microbiome by activating pathways that preferentially target particular  
88 groups of microbes. The copy number of gene families containing Toll/Interleukin  
89 Repeat (TIR) domains in particular, have received special attention as a possible  
90 influence on microbiome structure<sup>26</sup>. TIR domains are a key intracellular signaling  
91 domain, found in multiple innate immune gene families, such as Toll-like Receptors  
92 (TLR), Interleukin-1 Receptors (IL-1R), coral-specific TIR-only genes of unknown  
93 function, and Myeloid Differentiation Factor 88 (myD88). Collectively, these genes are  
94 known as TIR-domain containing genes<sup>27</sup>. The genomic copy number of some gene  
95 families of TIR-domain containing genes is known to vary greatly between coral species,  
96 and on this basis these genes have been hypothesized to influence cross-species  
97 differences in coral microbiome structure<sup>26</sup>. However, a lack of consistently collected  
98 cross-species microbiome data has so far precluded empirical testing of this intriguing  
99 idea.

100  
101 In this study we tested whether dramatic changes in the copy number of coral TLR or IL-  
102 1R gene families have driven corresponding changes in microbiome richness, evenness,  
103 or composition during more than 250 million years of scleractinian coral evolution. Our  
104 analysis combined genomic analysis of all major lineages of scleractinian coral for which  
105 genomes are publicly available with data on coral mucus, tissue, and endolithic skeleton  
106 microbiomes from the Global Coral Microbiome Project (GCMP) dataset<sup>3</sup> — a collection  
107 of more than 1440 16S rRNA libraries from diverse coral species. We then used  
108 established phylogenetic comparative methods to test whether coral species' TLR or IL-  
109 1R gene families correlated with their microbiome structure or composition. The results  
110 identify potential drivers of microbiome structure among sequenced corals, and highlight  
111 the value of comparative analysis for supporting or refuting whether specific host traits  
112 underlie differences in microbiome structure between animal species. They further  
113 support the idea that different regions of coral anatomy differ not just in microbiome  
114 composition, but also in responsiveness to host traits — with the parts of the coral that  
115 are most strongly linked to host traits sometimes being a surprise.

## 116 **Methods**

### 117 **Genomic Data Acquisition**

118 Reference coral genomes were selected based on completeness and overlap with the  
119 Global Coral Microbiome Project dataset. Twelve coral genomes were downloaded from  
120 NCBI (<https://www.ncbi.nlm.nih.gov/>) and Reef Genomics (<http://reefgenomics.org>). A  
121 list of urls for the genomes can be found in **Table S1A**.

122

### 123 **Domain Annotation**

124 The downloaded coral genomes were used to locate TIR, leucine rich repeats (LRR), and  
125 immunoglobulin (Ig) containing genes using a custom pipeline found on github

126 ([https://github.com/zaneveld/GCMP\\_genomics](https://github.com/zaneveld/GCMP_genomics)). Genome analysis occurred in two steps.  
127 First, genomes were analyzed using TransDecoder (v5.5.0)  
128 (<https://github.com/TransDecoder/TransDecoder/wiki>) to identify candidate coding  
129 regions within the genome files. During this process, TransDecoder converts the  
130 nucleotide sequences in the genome file to possible amino acid sequences using different  
131 open reading frames needed to conduct this translation. The peptide file generated from  
132 TransDecoder was next searched with HMMER ([hmmer.org](http://hmmer.org), HMMER 3.3.2 (November  
133 2020)) to locate putative TIR domains as well as known TIR-associated domains. The  
134 TIR, LRR, and Ig associated peptide alignment files used in this search were downloaded  
135 from the Pfam website (<http://pfam.xfam.org/>). These 14 alignment files used are found  
136 in **Table S2B, C**. The Pfam domain alignment files were used to build profiles in  
137 HMMER using hmmbuild by reading in the alignment file and creating a new Hidden  
138 Markov Model (HMM) profile. The HMM profiles were then used to search the  
139 TransDecoder peptide files. The output file from hmmscan contained significant matches  
140 between the HMM profile and the transdecoder peptide file. The resultant hmmscan file  
141 was used to count the number of TIR-domain containing sequences found for each  
142 organism.

143  
144 TIR-domain containing genes were further subdivided by scanning each for LRR or Ig  
145 domains using the same procedure. TIR-domain-containing genes were then subdivided  
146 into categories based on their domains: TIR only (defined by TIR domain and no LRR or  
147 Ig domains), TLR (TIR and one or more LRR domains), and IL-1R (TLR and one or  
148 more Ig domains) genes. Numbers of each type of gene, and average numbers of Ig or  
149 LRR domains within each type of gene were used in further analysis.

150  
151 **Coral sampling and microbiome analysis**  
152 The Global Coral Microbiome Project (GCMP) coral mucus, tissue and skeleton samples  
153 reanalyzed here were originally collected and processed following the methods outlined  
154 in Pollock *et al.*, 2018<sup>3</sup>. Those methods are briefly restated here. All coral samples were  
155 collected by AAUS-certified scientific divers, in accordance with local regulations. These  
156 plus additional international samples were then resequenced with protocols standard for  
157 the Earth Microbiome Project<sup>28</sup>. Bacterial and archaeal DNA were extracted using the  
158 PowerSoil DNA Isolation Kit (MoBio Laboratories, Carlsbad, CA; now Qiagen, Venlo,  
159 Netherlands). To select for the 16S rRNA V4 gene region, polymerase chain reaction  
160 (PCR) was performed using the following primers with illumina adapter sequences  
161 (underlined) at the 5' ends: 515F<sup>29</sup> 5'- TCG TCG GCA GCG TCA GAT GTG TAT  
162 AAG AGA CAG GTG YCA GCM GCC GCG GTA A -3' and 806R<sup>30</sup> 5'- GTC TCG  
163 TGG GCT CGG AGA TGT GTA TAA GAG ACA GGG ACT CAN VGG GTW TCT  
164 AAT -3'. PCR, library preparation and sequencing on an Illumina HiSeq (2x125bp) was  
165 performed by the EMP<sup>28,31</sup>. The resulting 16S rRNA amplicon sequences from the  
166 GCMP are available in the Qiita database Qiita (CRC32 id: 8817b8b8 and CRC32 id:  
167 ac925c85). Metadata for all GCMP samples are available in **Table S1B**.

168  
169 **16S library preparation, sequencing, and initial quality control**  
170 16S rRNA sequencing data were processed in Qiita<sup>32</sup> using the standard EMP workflow.  
171 Briefly, sequences were demultiplexed based on 12bp Golay barcodes using

172 “split\_libraries” with QIIME 1.9.1 default parameters<sup>33</sup> and trimmed to 100bp to remove  
173 low quality base pairs. Quality control (e.g., denoising, de-replication and chimera  
174 filtering) and identification amplicon sequence variants (ASVs) were performed using  
175 deblur 1.1.0<sup>34</sup> with default parameters. The resulting biom and taxonomy tables were  
176 obtained from Qiita (CRC32 id: 8817b8b8 and CRC32 id: ac925c85) and processed using  
177 a customized QIIME2 v. 2020.8.0<sup>35</sup> pipeline in python  
178 (github.com/zaneveld/GCMP\_global\_disease).

179

#### 180 **Mitochondrial annotation and quality control**

181 Taxonomic assignment of ASVs was performed using vsearch<sup>36</sup> using a modified version  
182 of the SILVA v. 138<sup>37</sup> taxonomic reference. The sole change to the SILVA138 reference  
183 was supplementation with additional coral mitochondrial reads obtained from metaxa2<sup>38</sup>.  
184 In benchmarks, this change greatly improves annotation of coral mitochondrial rRNAs,  
185 without increasing false positive taxonomic assignments<sup>39</sup>. This expanded taxonomy is  
186 referred to as “silva\_metaxa2” in code. After taxonomic assignment, all mitochondrial  
187 and chloroplast reads were removed (**Table S3**).

188 The bacterial phylogenetic tree was built using the SATé-enabled phylogenetic placement  
189 (SEPP) insertion technique with the q2-fragment-insertion plugin<sup>40</sup>, again using the  
190 SILVA v. 138<sup>37</sup> database as reference taxonomy. The final output from this pipeline  
191 consisted of a taxonomy table, ASV feature table and phylogenetic tree that were used for  
192 downstream analyses.

193

194 Phylogenetic comparison of innate immune gene repertoire and microbiome richness  
195 Genome TIR domains were compared to the microbiome data collected from the GCMP.  
196 The  $\alpha$  and  $\beta$ -diversity of the microbial community were compared to the TIR, TLR, and  
197 IL-R domain copy numbers using phylogenetically independent contrasts (PICs) with the  
198 phytools package in R. PICs use the coral species phylogenetic information in  
199 comparison with the TIR-associated domains and ASV and Gini Index information to  
200 assess the relatedness for  $\alpha$ -diversity. PIC analysis for phylogenetic  $\beta$ -diversity metrics  
201 (Weighted and Unweighted UniFrac) were created from three PC axes (PC1, PC2, and  
202 PC3) of a PCoA ordination. Analyses were conducted on all three axes. The PIC method  
203 takes into account a priori the importance of phylogenetic history on trait variation when  
204 extracting information in relation to the common ancestor. Code used for this analysis is  
205 found on github.

206

#### 207 **Microbial taxonomic analysis**

208 Microbial taxonomic analysis was conducted using the ANCOM-BC package in phyloseq  
209 in R<sup>41</sup>. Analyses were conducted at the class and family level with relation to IL-1R and  
210 TLR copy numbers. Lists of significant microbes were generated for mucus, tissue,  
211 skeleton, and all compartments. Heatmaps were generated to visualize positive and  
212 negative correlation of the microbial community.

213

214

215 **Results**

216

217 Sequenced coral genomes vary greatly in TIR-domain containing gene copy number.  
218 Previous analyses have reported significant variation in the copy number of TIR-domain  
219 containing genes among coral genomes. We annotated the genomic copy number of TIR-  
220 domain containing genes in 11 coral genomes that were also represented in microbiome  
221 data from the Global Coral Microbiome Project (GCMP) (**Table S1**). While some prior  
222 studies have analyzed both genomes and transcriptomes in order to maximize discovery  
223 of new TLR or IL-1R homologs, we chose to exclude transcriptomes from our analysis in  
224 order to prevent any potential confounding effects of some innate immune genes not  
225 being expressed in transcriptomes. As a result of these annotations (Methods), we  
226 identified numerous TLR, IL-1R and TIR-only genes (**Table S2, 4**). Despite these  
227 methodological differences, our annotations mostly agree in trend and rank with prior  
228 studies of coral innate immune repertoires<sup>26,42</sup>.

229

230 Many innate immune genes have modular structures based on the domains that they  
231 contain, and TIR domains commonly co-occur with several other domains within innate  
232 immune genes. We further subdivided TIR-domain containing genes based on the other  
233 domains present: genes with both TIR and immunoglobulin (Ig) domains were annotated  
234 as interleukin-1 receptors (IL-1R) while genes with both TIR domains and leucine rich  
235 repeat (LRR) domains were annotated as toll-like receptors (TLR) (**Fig. 1**). We also  
236 analyzed the total count of TIR domains, regardless of which gene they were part of and  
237 the presence or absence of other co-associated domains.

238

239 In keeping with past work<sup>26,42</sup>, we find that both the copy number of TLR, IL-1R and  
240 TIR-only genes, and the total abundance of their component TIR, LRR and Ig domains  
241 varies greatly across coral genomes (**Table 1**).

242

243 **Coral IL-1R and TLR gene family copy number correlate with overall microbiome  
244 richness and evenness.**

245 In order to determine whether TLR or IL-1R might regulate microbiome biodiversity, we  
246 used phylogenetic independent contrasts (PIC) analysis to correlate changes in the  
247 genomic copy number of IL-1R and TLR against changes in microbiome richness or  
248 evenness during coral evolution.

249

250 We measured microbiome richness as the natural log of the observed number of amplicon  
251 sequence variants (ASVs) per 1000 sequences (**Table S5A**) (see Methods). Microbiome  
252 richness was significantly reduced by increases in the copy number of IL-1R (PIC  $R^2 =$   
253 0.835,  $q_{FDR} = 0.00055$ ; **Fig. 2B, D; Fig. S1C, D; Table S6A**), or TLR (PIC  $R^2 = 0.707$ ,  
254  $q_{FDR} = 0.0076$ ; **Fig. 2 C, D; Fig. S1E, F; Table S6A**). Thus, corals that harbor more TLR  
255 or IL-1R gene copies tend to have less diverse microbiomes, and vice versa. In manual  
256 inspection of the data, there were several striking examples of this statistical trend (**Table**

257 **S7).** In the genus *Porites*, *P. lutea* had more than twice as many IL-1R and TLR gene  
258 copies as the closely related *P. rus* (14 IL-1R copies and eight TLR gene copies in *P.*  
259 *lutea* vs. six IL-1R copies and two TLR copies in *P. rus*; **Table 1**). Consistent with the  
260 idea that *P. lutea*'s expanded gene repertoire may play a role in microbiome filtering, *P.*  
261 *lutea*'s microbiome was roughly half as diverse as that of *P. rus* (56 ASVs/1000 reads vs.  
262 114 ASVs/1000 reads, across all sample types).

263  
264 We also quantified the microbiome evenness of each coral species in the analysis using  
265 the Gini Index (**Table S5B**), which takes on its highest value when ecological  
266 communities are least even. Gini index scores were strongly and significantly negatively  
267 correlated with the genomic copy number of IL-1R genes (PIC  $R^2 = 0.876$ , qFDR =  
268 0.000357; **Fig. S5C, D; Table S6A**) and TLR genes (PIC  $R^2 = 0.805$ , qFDR = 0.0014; **Fig.**  
269 **S5E, F; Table S6A**), indicating that corals with more IL-1R or TLR gene copies have  
270 higher evenness.

271  
272 These results support the prior hypothesis that IL-1R and TLR gene family expansions  
273 may influence coral microbiome structure. The magnitude of the effect was, however,  
274 quite surprising, with IL-1R gene copy number explaining ~83% of the variation in  
275 microbiome richness, and ~88% of the variation in microbiome evenness, among coral  
276 species in the analysis. Although necessarily limited to coral species for which genomes  
277 are available, these correlations are much stronger than the effects of several biotic and  
278 abiotic factors in the same GCMP dataset, including depth, temperature, and turf-algal  
279 contact<sup>3</sup>.

280  
281 **Endolithic skeleton microbiomes drive correlations between TLR and IL-1R gene**  
282 **family expansion and microbiome structure.**

283 To this point, all our results were conducted by correlating genomic features of corals  
284 against the overall microbiome diversity of all available microbiome samples from each  
285 species in the GCMP dataset. However, microbiome richness has been shown to vary  
286 between coral compartments<sup>3</sup>. We expected that host tissues — where the immune  
287 system could most obviously act — would have microbiomes that most closely correlate  
288 with the innate immune gene repertoire of the host.

289  
290 To test this idea, we separated coral microbiome samples into those that derive from  
291 mucus, tissue or endolithic skeleton, and repeated tests for correlations between coral  
292 innate immune repertoires and microbiome richness and evenness within each of those  
293 regions of anatomy.

294  
295 Contrary to our hypothesis, coral endolithic skeleton — not tissue or mucus — was the  
296 sole driver of correlations between coral innate immune repertoire and microbiome  
297 richness (**Fig. 2E-G; Fig. S1-4; Table S6, 8**) and evenness (**Fig. S5-8; Table S6, 8**).  
298 Microbiome richness in coral endolithic skeleton was significantly correlated with IL-1R  
299 ( $R^2 = 0.944$ , qFDR =  $2.05 \times 10^{-5}$ ; **Fig. 2F, Fig. S4C, D; Table S6D**), and TLR ( $R^2 =$   
300  $0.90798$ , qFDR =  $9.36 \times 10^{-5}$ ; **Fig. 2G; Fig. S4E, F; Table S6D**) gene copies, whereas  
301 tissue (**Fig. S3; Table S5C**) and mucus (**Fig. S2; Table S6B**) microbiome richness was  
302 not. Microbiome evenness showed similar patterns (**Fig. S6-8; Table S6, 8**).

303 Previous studies have reported that coral endolithic skeleton microbiomes are more  
304 species-rich than mucus or tissue, and show both species-specificity and signals of  
305 phylosymbiosis with their coral hosts<sup>3</sup>. Our results further suggest that endolithic skeleton  
306 microbiome diversity has tracked gene family expansions or contractions of coral TLR  
307 and IL-1R genes over evolution.

308

309

310 **Microbiome composition varies with IL-R and TLR gene copy numbers.**

311 In addition to regulating microbiome richness and evenness, coral innate immune systems  
312 may also influence coral microbiome composition. If so, we might expect microbiome  
313 composition to correlate with the repertoire of innate immune proteins encoded in coral  
314 genomes. To test this, we compared differences in overall microbiome composition for  
315 each pair of coral species using two phylogenetic beta diversity metrics: Weighted  
316 UniFrac and Unweighted UniFrac. Using these beta-diversity distance metrics, we  
317 conducted principal coordinates analysis (PCoA), using the first three PC axes (PC1, PC2,  
318 and PC3) of the PCoA ordination (Methods). We correlated the microbiome PC  
319 coordinates against the number of predicted TLR or IL-1R gene copies (**Fig. 3; Table**  
320 **S9**).

321

322 Innate immune gene copy numbers strongly and significantly correlated with microbiome  
323 composition. When all samples were considered together (irrespective of anatomical  
324 compartment) Weighted UniFrac PC1 correlated strongly with the genomic copy number  
325 of IL-1R genes (PIC Weighted UniFrac PC1  $R^2 = 0.917$ ,  $q_{FDR} = 0.00012$ ; **Fig. 3A, C, D;**  
**Table S9A**) and TLR genes (PIC Weighted UniFrac PC1  $R^2 = 0.77$ ,  $q_{FDR} = 0.0028$ ; **Fig.**  
326 **3B, E, F; Table S9A**). Unweighted UniFrac PC1 showed similar trends (**Table S9A**).  
327 These results indicate that gene family expansions or contractions of the TLR and IL-1R  
328 gene families over evolution corresponded to dramatic changes in overall microbiome  
329 composition.  
330

331 We repeated the above protocol separately on the mucus, tissue, and skeleton  
332 compartments separately (**Table S9B-D**). In coral mucus, tissue and skeleton, IL-1R gene  
333 copy number significantly correlated with Weighted UniFrac PC1 of the microbiome  
334 ( $PIC R^2 = 0.72-0.81$ ,  $FDR q < 0.01$ ; **Table S9A-C**). TLR gene copy number significantly  
335 correlated with Weighted UniFrac PC1 in coral mucus and tissue ( $PIC R^2 = 0.73$ ,  $q_{FDR} =$   
336  $0.004$ ; **Table S9B, C**) but not endolithic skeleton (**Table S9D**). In qualitative  
337 (presence/absence) analysis of microbiome  $\beta$ -diversity, IL-1R gene copy number  
338 correlated with Unweighted UniFrac PC1 in coral tissue and skeleton compartments, but  
339 not mucus (**Table S9B-D**), while TLR gene copy number correlated with Unweighted  
340 UniFrac PC1 in coral tissue but not mucus or skeleton (**Table S9B-D**).

341

342 These  $\beta$ -diversity results were more complex than the straightforward pattern of  
343 associations between innate immune gene copy number and microbiome richness. In  
344 coral tissue both IL-1R gene copy number and TLR gene copy number correlated with  
345 key aspects of quantitative (Weighted UniFrac PC1) and qualitative (Unweighted  
346 UniFrac PC1) microbiome  $\beta$ -diversity, in keeping with our original expectation that  
347 immunity should act strongly on the tissue-associated microbiome. In mucus, both TLR  
348 and IL-1R gene copy numbers appeared correlated with microbiome  $\beta$ -diversity when

349 using quantitative but not qualitative metrics, suggesting immunity might influence  
350 microbial relative abundance more strongly than microbial presence/absence. In skeleton,  
351 IL-1R appeared correlated with IL-1R gene copy number, but not TLR gene copy number  
352 regardless of  $\beta$ -diversity metric. Together, these results suggest anatomically specific  
353 correlations between gene family expansion of some key innate immune genes and  
354 microbiome  $\beta$ -diversity.

355

356 **IL-1R and TLR copy number is associated with differential abundance of key  
357 microbes.**

358 We sought to identify microbial taxa that may be influenced by IL-1R or TLR gene copy  
359 number. This analysis could be confounded by the compositional nature of coral  
360 microbiome data. Therefore ANCOM-BC<sup>41</sup>, which accounts for compositionality, was  
361 used for the analysis. We first tested whether IL-1R copy number correlated with  
362 microbial differential abundance in all samples regardless of tissue compartment (i.e.  
363 ‘all’). In this overall analysis, IL-1R copy number correlated with the differential  
364 abundance of 102 families of bacteria and archaea, while TLR copy number correlated  
365 with 88 families (**Table S10A**).

366 Correlations between microbiome composition and IL-1R or TLR copy number varied  
367 with anatomy. The abundance of 38 bacterial families were significantly correlated with  
368 TLR copy number (ANCOM-BC qFDR < 0.05 in mucus, tissue, and skeleton; **Tables**  
369 **S10B-D; Fig. S11-S13**) and 38 bacterial families were also significantly and consistently  
370 correlated with IL-1R copy number (ANCOM-BC qFDR < 0.05 in mucus, tissue, and  
371 skeleton; **Table S10B-D**; raw heatmaps in **Fig. S14-S16**), both regardless of  
372 compartment. In contrast to the bacterial families with consistent interrelationships, some  
373 were specific to one or more compartments. One example are Rickettsiaceae, which live  
374 intracellularly in host cells. Rickettsiaceae relative abundance in tissue decreased with IL-  
375 1R (ANCOM-BC coef = -0.011, W = 0.33, qFDR = 0; **Fig. 4, Fig. S15; Table S10C**) and  
376 TLR (ANCOM-BC coef = -0.028, W = 1.36, qFDR = 0; **Fig. 4, Fig S12, Table S10C**), but  
377 this taxon was not present in mucus (**Fig. S11, Fig S14**) or skeleton (**Fig. S13, Fig. S16**).  
378 *Nitrosopumiliaceae* archaea were notable for correlating with IL-1R and TLR gene copy  
379 number across all compartments (all ANCOM-BC qFDR < 0.05; **Fig S11-S16**).  
380

381

382 **The domain architecture of TLR but not IL-1R genes is associated with microbiome  
richness.**

383 IL-1R and TLR genes are known to vary in the domain architecture of their extracellular  
384 regions, with variable numbers of Ig or LRR sensing domains, respectively. We reasoned  
385 that if higher copy numbers of TLR or IL-1R genes are associated with microbiome  
386 richness because they act as filters on the microbiome, the same selective pressures (for  
387 greater specificity in microbial associates) might also influence the domain architecture  
388 of extracellular sensing components within TLR or IL-1R genes. To test this, we  
389 analyzed the average number of LRR and Ig domain copy numbers associated with each  
390 TLR or IL-1R gene in each coral species.  
391

392

393 Interestingly, we find that there is a significant positive correlation between LRR domain  
394 copy number per TLR genes and TLR copies ( $R^2 = 0.437$ ,  $p = 0.0159$ ; **Fig. 5A, B; Fig.**  
**S9A**) but not Ig copy number with IL-1R ( $R^2 = 0.00067$ ,  $p = 0.345$ ; **Fig. 5C, D; Fig.**

395 **S9B**). In other words, corals with more TLR genes also have TLR genes with more LRR  
396 domains each.

397

398 Furthermore, we find that microbiome richness is correlated negatively with the average  
399 number of LRR domain copies ( $\text{PIC } R^2 = 0.748$ ,  $p = 0.00059$ ; **Fig 5B**) but not Ig domain  
400 copies ( $\text{PIC } R^2 = 0.341$ ,  $p = 0.059$ ; Fig 5D). That is, corals whose TLR genes typically  
401 have more elaborate domain architectures also tend to have simpler (or more specific)  
402 microbial associations. Importantly, the genomic copy number of LRR or Ig domains in  
403 total (rather than per gene) did not correlate with microbiome richness and beta diversity  
404 (**Table S8, S11**), so this finding does not simply recapitulate our previous findings  
405 regarding gene copy number.

406

#### 407 **Responses to IL-1R and TLR are correlated between bacterial families.**

408 The microbe associated molecular patterns (MAMPs) detected by species-specific  
409 members of the TLR and IL-1R gene families could in principle be the same or  
410 independent. If independent, the correlation between any given microorganism and TLR  
411 gene family expansions would be independent of IL-1R gene family expansions. To test  
412 this, we analyze whether the correlation coefficients between each microbial family's  
413 relative abundance with TLR or IL-1R copy number were themselves correlated with one  
414 another. Microbial families' responses to IL-1R and TLR gene family copy numbers  
415 were themselves very strongly correlated ( $R^2 = 0.9062$ ; **Fig S11**). Thus, microbes that are  
416 in high abundance in corals with many IL-1R gene copies also tend to be in high  
417 abundance in corals with many TLR gene copies. This suggests that TLR and IL-1R gene  
418 family expansions sculpt coral microbiomes in similar, rather than contrasting ways.

## 419 **Discussion**

420 By combining coral microbiome and genomic data in a comparative framework, we  
421 demonstrate that TIR-domain containing innate immune gene repertoires strongly  
422 correlate with microbiome structure and diversity. These results suggest that gene family  
423 expansions of innate immune genes may have contributed to differences in the structure  
424 of coral microbiomes across millions of years of evolution. Those differences in  
425 immunity and microbiome structure, in turn, may influence the ability of modern  
426 scleractinian corals to survive escalating challenges from disease and climate change.  
427

#### 428 **Coral innate immune systems may be filtering microbiome membership.**

429 A key finding of the Earth Microbiome Project was that the diverse communities of  
430 microbes associated with animals and plants are nonetheless much less diverse than most  
431 environmental microbiomes<sup>28</sup>. Indeed, these animal-associated microbiomes were found  
432 to show high nestedness relative to the environment, indicating that what lives on animals  
433 is mostly — though certainly not entirely — a subset of environmental microbes<sup>28</sup>. This  
434 suggests that filtering of environmental microbes is one key process shaping animal and  
435 plant microbiomes. That filtering is likely to be genetically encoded, since more closely  
436 related animals tend to have more similar microbiomes ('phylosymbiosis'<sup>3,43–45</sup>),  
437 excepting important deviations from this trend such as those driven by the evolution of

438 specialized diets<sup>46,47</sup> or flight<sup>48</sup>. Could evolutionary changes in host immunity drive this  
439 trend, by altering which environmental microbes are excluded?  
440  
441 Our results in corals suggest that, for this group at least, immunity plays an important role  
442 in overall microbiome richness and evenness. Both coral microbiome composition<sup>3</sup>, and  
443 coral innate immune responses<sup>49,50</sup> have long been known to vary between species.  
444 Within coral populations, there is evidence that variation in immune activity between  
445 coral fragments correlates with their microbiome structure. For example, in *Montipora*  
446 *capitata*, increases in phenoloxidase activity correlated with decreased microbiome  
447 richness<sup>51</sup>. If such correlations extended across species, it could begin to explain why  
448 coral microbiomes differ so greatly in bacterial and archaeal biodiversity.  
449 TIR-domain containing genes have undergone large gene-family expansions in some  
450 lineages of corals, which has been proposed as a driver of differences in coral  
451 microbiome richness<sup>26</sup>. Our findings support this hypothesis, and suggest that expansions  
452 of key innate immune genes reduce microbiome richness by allowing for sensing and  
453 exclusion of more diverse groups of microbes.  
454

455 **Microbiome composition changes with TLR and IL-1R copy number**  
456 We find a relationship between microbiome  $\beta$ -diversity and the copy number of TIR-  
457 containing innate immune genes. Immune genes of animals and plants have in the past  
458 been reported to alter the  $\beta$ -diversity of symbiotic microbes, including commensals. For  
459 example, using Toll-like receptor (TLR) 5 deficient compared to wild type mice, TLR  
460 genes have been correlated with membership and host-microbial interactions with  
461 specific members of the mouse gut microbiome, although the overall effect of TLR on  
462 gut microbiome  $\beta$ -diversity remains controversial<sup>52</sup>. Similarly, *Arabidopsis* with loss of  
463 function mutations in the pattern recognition receptor (PRR) gene FLS2, have altered  
464 rhizosphere microbiome  $\beta$ -diversity relative to wild type controls<sup>53</sup>. Our findings extend  
465 these observations to coral microbiomes, and suggest that differences in innate immunity  
466 may explain substantial portions of the known differences in microbiome structure  
467 between coral species.  
468  
469 In our results, the relative abundances of diverse microbial taxa correlated with TLR or  
470 IL-1R gene copy number. Interestingly, these effects were not independent: microbes that  
471 correlated with TLR copy number also tended to be correlated with IL-1R copy number.  
472 This might reflect either that TLR and IL-1R gene family expansions are driven by  
473 similar selective pressures and therefore tend to co-occur, or that both types of gene  
474 family expansion influence the microbiome in similar ways.

475  
476 **The relationship between innate immune gene repertoire and the microbiome is**  
477 **anatomically-specific**  
478 While there are clear reasons to expect coral innate immune gene repertoire to affect  
479 tissue-associated coral microbiomes, our results suggest that these gene family  
480 expansions have even more clear-cut effects on coral's endolithic skeleton microbiomes.  
481 Corals show compartmentalized differences in molecular function<sup>54</sup> and microbial  
482 richness and composition across anatomy<sup>3</sup>. Perhaps surprisingly, the microbiome of coral  
483 endolithic skeleton has been shown to be far more diverse than coral tissues or mucus<sup>3</sup>. In

484 our results, endolithic skeleton microbiomes were more strongly correlated with host  
485 innate immunity than either mucus or tissue.

486  
487 These results suggest that coral immunity strongly influences endolithic microbiomes.  
488 They also underline the importance of efforts to reevaluate how we conceptualize coral  
489 immunity and calcification. While coral calcification and immunity are typically thought  
490 of separately, recent work synthesizes these two fields<sup>55</sup>, noting that skeleton is a key  
491 barrier against pathogens, and in many species contains diverse defensive chemical  
492 compounds and enzymes. These notably include melanin, which is a key aspect of  
493 immune defense in many non-vertebrate lineages.

494  
495 **Disease-susceptible corals have more, not fewer, TIR-domain containing genes.**  
496 One counter-intuitive aspect of our results is that the coral taxa with the largest numbers  
497 of TIR-containing innate immune genes tend to be those, such as *Acropora*, regarded as  
498 more susceptible to disease<sup>56</sup>. This is surprising, because we might expect more disease-  
499 susceptible coral species to have less diverse innate immune gene repertoires. How gene-  
500 family expansion, the commensal microbiome, and coral disease interact is a rich topic  
501 for future investigation. Our results here suggest several hypotheses that could be  
502 explored. It could be that more diverse microbial ecosystems are less susceptible to  
503 invasion by pathogens, as per Elton's 1958 biotic resistance hypothesis<sup>57,58</sup>. Alternatively,  
504 less rich microbiomes may be less functionally redundant, increasing the risk that loss of  
505 any particular beneficial microbe may degrade host health<sup>59,60</sup>. Finally, the damage  
506 threshold hypothesis<sup>61</sup> proposes that corals differ in immune strategy, with many slow-  
507 growing corals constitutively expressing a variety of innate immune genes, while other  
508 fast-growing corals adopt a reactive strategy, which avoids expending resources on  
509 baseline expression of many innate immune genes in order to maximize growth or  
510 fecundity. If so, then reactive, fast-growing corals may experience stronger selective  
511 pressures to diversify sensors that can detect pathogens or cellular damage, since their  
512 baseline level of protection is low. TIR-domain containing gene family expansions in  
513 these reactive corals may enable more sensitive and/or specific responses to pathogen  
514 exposure.

515  
516 **Conclusions**  
517

518 We find that among sequenced coral genomes, gene family expansions of TLR and IL-1R  
519 genes are correlated with alterations in microbiome structure, and reductions in  
520 microbiome richness — with this apparent interplay between innate immunity and the  
521 microbiome most noticeable in coral endolithic skeleton. These findings are consistent  
522 with the idea that animal immunity sculpts microbiome structure and composition in part  
523 by sensing and filtering out many environmental microbes. This interpretation of the  
524 correlations we found between gene copy number and the microbiome is reinforced by  
525 the correlation between microbiome richness and the domain architecture within TLR  
526 genes, wherein there are more sensing (i.e. LRR) domains per TLR gene in corals that  
527 have lower microbiome richness. Our results further underscore the importance of  
528 distinguishing coral microbiomes across anatomy, and of exploring how coral innate  
529 immunity regulates corals' diverse endolithic microbiomes. Finally, these results

530 emphasize that integrating expanding coral genome and microbiome datasets in  
531 comparative frameworks is a promising approach that will help to uncover the  
532 interactions between immunity, the microbiome, and reef health.

### 533 **Data Availability**

534 Biom and taxonomy tables are available on Qiita (Study ID 10895). Analysis code is  
535 available on GitHub: [https://github.com/zaneveld/GCMP\\_Genomics/](https://github.com/zaneveld/GCMP_Genomics/)

### 536 **Acknowledgements**

537 The authors would like to acknowledge many contributors for their field assistance  
538 during past collections of Global Coral Microbiome Project data reanalyzed in this  
539 manuscript, including: Rebecca Vega Thurber, a leader of the original GCMP project;  
540 Tasman Douglass, Margaux Hein, Frazer McGregor, Kathy Morrow, Katia Nicolet,  
541 Cathie Page, and Gergely Torda for their field assistance in Australia; Valeria Pizarro,  
542 Mateo López-Victoria, Styles Smith, Alaina Weinheimer, Claudia Tatiana Galindo for  
543 Assistance in Colombia; Chris Voolstra, Maren Ziegler, Anna Roik, and many others at  
544 KAUST for field assistance in Saudi Arabia; Mark Vermeij, Kristen Marhaver, Pedro  
545 Frade, Ben Mueller, and others at CARMABI for field assistance during sampling in  
546 Curaçao; Danwei Huang for field assistance in Singapore; Ruth Gates, Katie Barrott,  
547 Courtney Couch, Keoki Stender for field assistance in Hawai'i; Le Club de Plongee  
548 Suwan Macha and Jean-Pascal Quod for field assistance, and Amelia Foster and Jerome  
549 Payet for sampling in Isle de la Réunion; the Burkepile lab for field assistance in  
550 Mo'orea; Yossi Loya, Raz Tamir for sampling assistance in Israel; and Lyndsy Gazda,  
551 Jamie Lee Proffitt, Gabriele Swain, and Alaina Weinheimer for their assistance in the  
552 laboratory. The authors also acknowledge the staff of the Coral Bay Research Station,  
553 Lizard Island Research Station, Lord Howe Island Marine Park, Lord Howe Island  
554 Research Station, and RV Cape Ferguson for their logistical support. This work was  
555 supported by a The GCMP dataset was supported by a National Science Foundation  
556 Dimensions of Biodiversity grant (#1442306) to Rebecca Vega Thurber and MM, with  
557 sequencing provided by an in-kind UC San Diego Seed Grant in Microbiome Science  
558 grant to JZ. Analysis in this manuscript was supported by NSF IoS CAREER grant (#  
559 1942647) and an in-kind UC San Diego Seed Grant in Microbiome Science grant to JZ.  
560 GCMP data collection was supported by a National Science Foundation Dimensions of  
561 Biodiversity grant (#1442306) to M.M.

### 562 **Author Contributions**

563 TB, DS, JZ analyzed the data; TB, JZ, DS wrote the manuscript; RM, JFP, MM, and JZ  
564 collected GCMP data and metadata; all authors edited the manuscript.

### 565 **Conflict of Interest Statement**

566 The authors declare no conflict of interest.

567  
568  
569

570

## 571 Tables

572

573 **Table 1.** TIR domain containing elements and their associated numbers per species

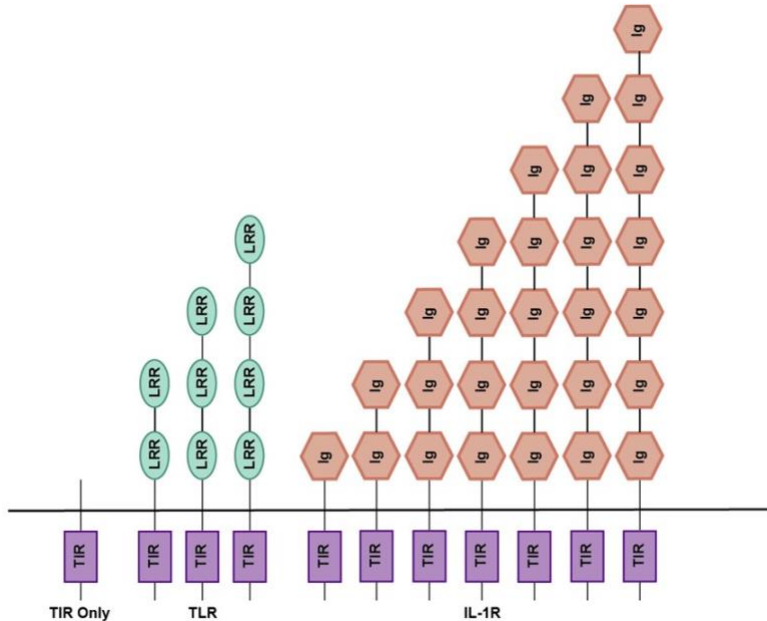
574

575

Coral Species	TIR Isoforms	IL-1R Copies	TLR Copies	Richness (ln ASVs /1000 reads)	Genome Sequence Reference
<i>Acropora hyacinthus</i>	37	11	8	3.788	Sinzato <i>et al</i> 2020
<i>Acropora cytherea</i>	33	10	7	3.619	Sinzato <i>et al</i> 2020
<i>Pocillopora damicornis</i>	24	6	5	4.368	Cunning <i>et al</i> 2018
<i>Pocillopora verrucosa</i>	28	7	7	4.369	Buitrago-Lopez <i>et al</i> 2020
<i>Orbicella faveolata</i>	27	7	6	4.484	Prada <i>et al</i> 2016
<i>Stylophora</i>	23	8	6	4.236	Chen <i>et al</i> 2008
<i>Galaxea fascicularis</i>	19	3	1	5.266	Ying <i>et al</i> 2018
<i>Porites lutea</i>	36	14	8	4.016	Robbins <i>et al</i> 2019
<i>Fungia fungites</i>	32	7	8	4.3	Ying <i>et al</i> 2018
<i>Montipora capitata</i>	27	5	1	4.034	Helmkampf <i>et al</i> 2019
<i>Porites rus</i>	29	6	2	4.739	Celis <i>et al</i> 2018

576

577

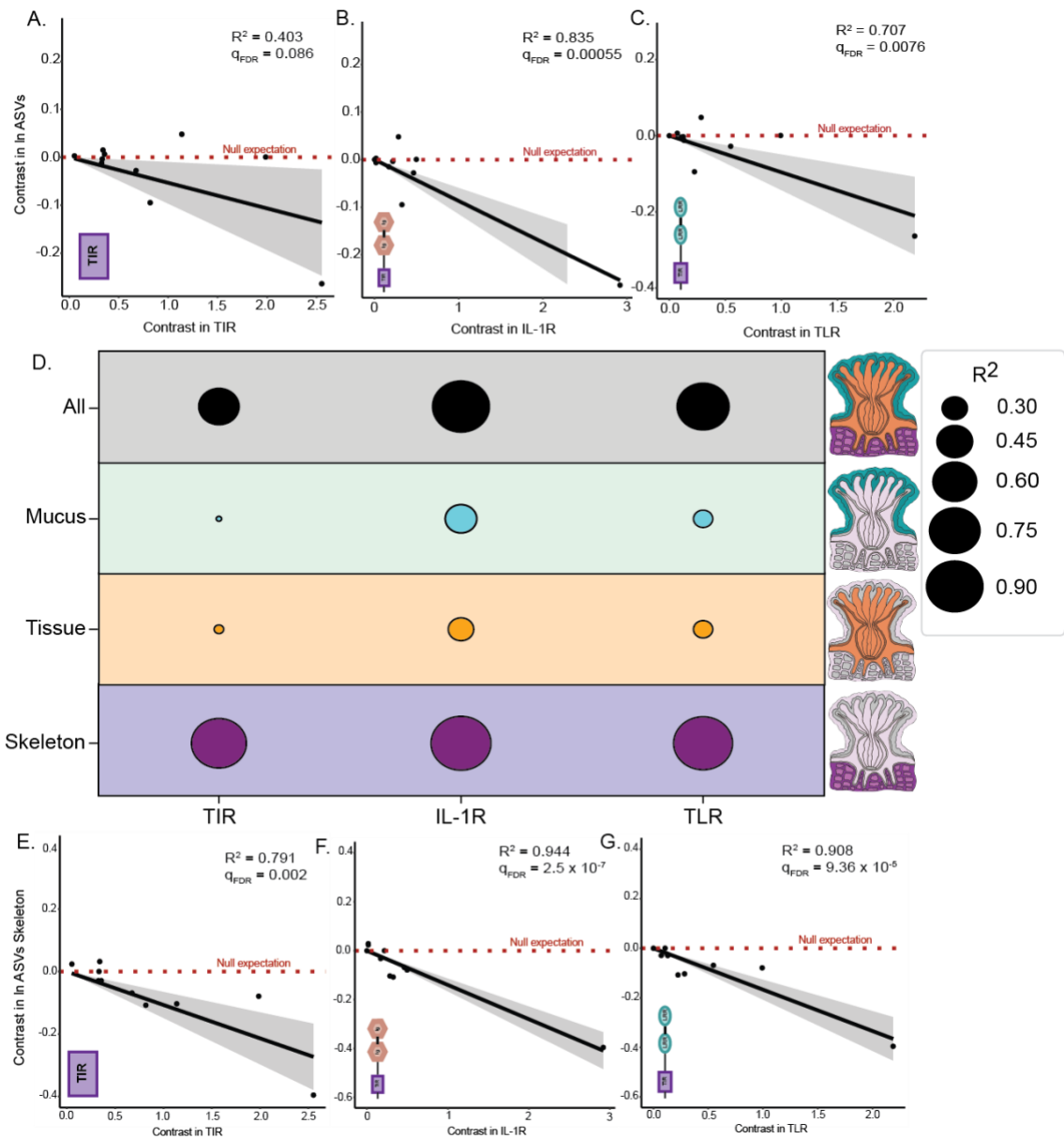
579 **Figures and Figure Legends**

580

581

582 **Fig. 1.** TIR containing gene architecture in coral genomes. Diagram depicts all domains  
 583 present in TIR only, TLR, or IL-1R genes identified in this study. TIR: Toll-Interleukin  
 584 Repeat; Ig: Immunoglobulin; LRR: Leucine Rich Repeat; TLR: Toll/Interleukin-like  
 585 Receptor; IL-1R: Interleukin-1 Receptor.

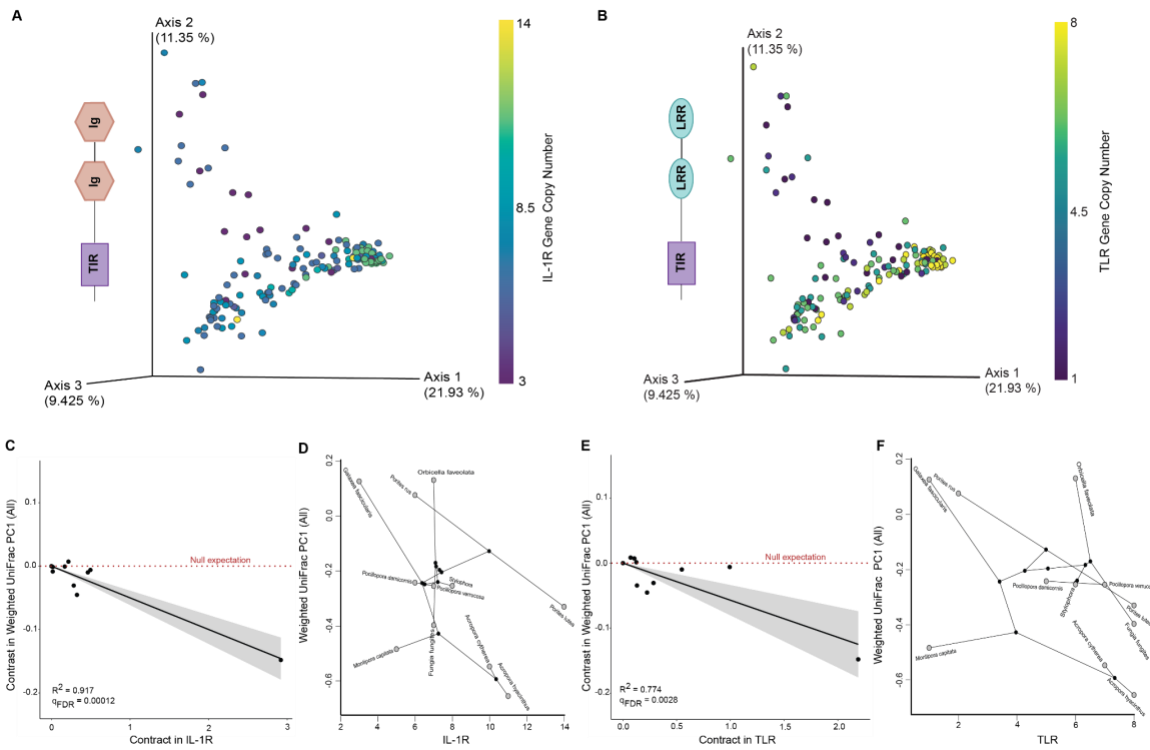
586



587  
588

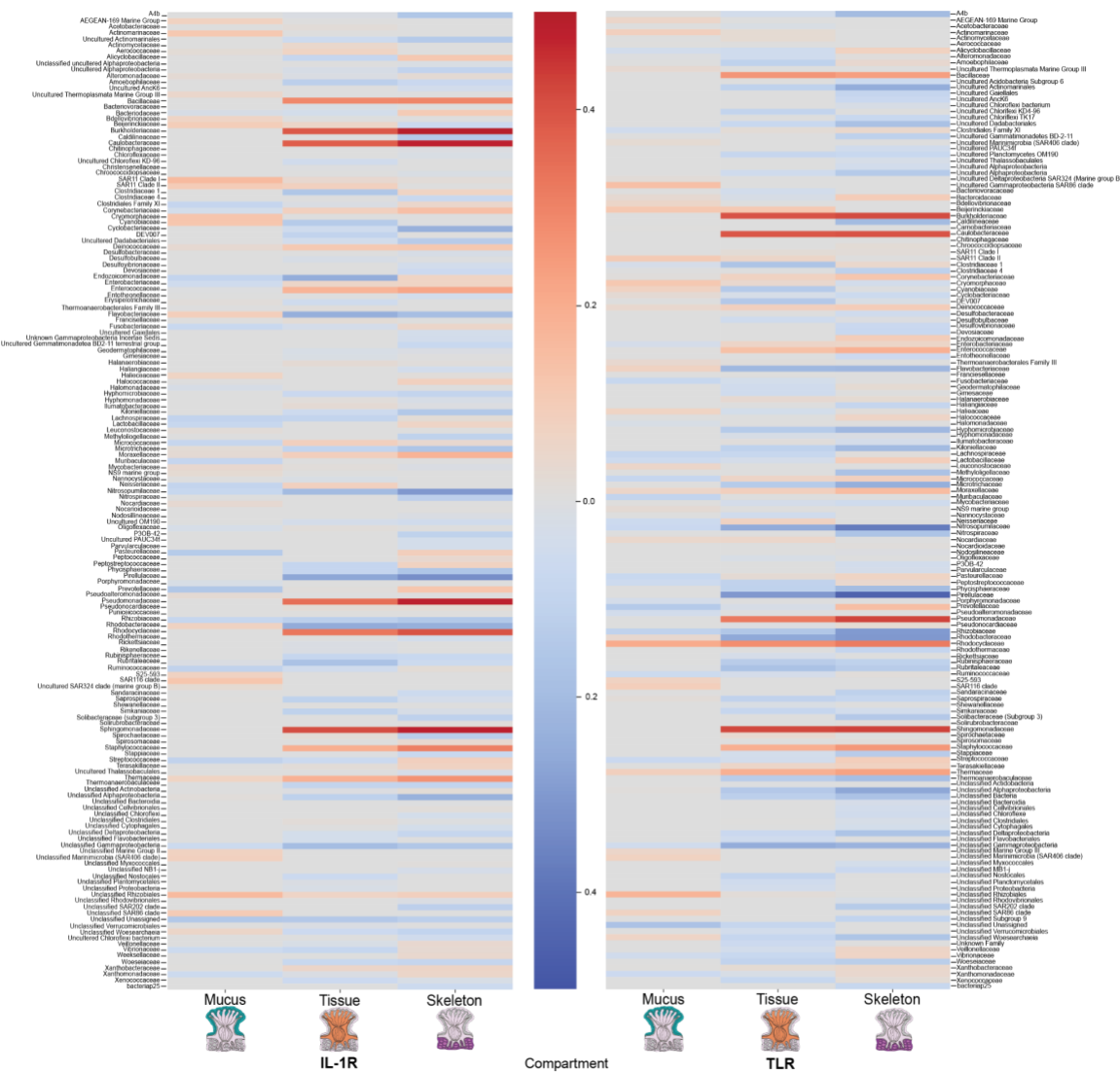
589 **Fig. 2.** Rows show phylogenetic independent contrast analysis of genomic copy number  
590 of innate immune components against log microbiome richness (ln ASVs), for all **A.** TIR  
591 domains ( $R^2 = 0.403$ ,  $q_{FDR} = 0.086$ ,  $p = 0.021$ ); **B.** IL-1R genes ( $R^2 = 0.835$ ,  $q_{FDR} =$   
592  $0.00055$ ,  $p = 5.13 \times 10^{-15}$ ); **C.** TLR genes ( $R^2 = 0.707$ ,  $q_{FDR} = 0.0076$ ,  $p = 0.0012$ ).  
593 Shading in phylogenetic independent contrasts analysis indicates the 95% confidence  
594 interval of the mean. **D.**  $R^2$  values from correlations of the genomic copy number of  
595 innate immune components against microbiome richness, organized by compartment.  
596 The bottom row uses microbiome data from coral skeleton only to show phylogenetic  
597 independent contrasts of innate immune components vs. log microbiome richness for: **E.**  
598 TIR-only genes ( $R^2 = 0.791$ ,  $q_{FDR} = 0.002$ ,  $p = 0.000252$ ); **F.** IL-1R genes ( $R^2 = 0.944$ ,  
599  $q_{FDR} = 2.15 \times 10^{-5}$ ,  $p = 6.39 \times 10^{-7}$ ); **G.** TLR genes ( $R^2 = 0.90798$ ,  $q_{FDR} = 9.36 \times 10^{-6}$ ,  
600  $p = 5.85 \times 10^{-6}$ ). No correlations had outliers, as defined by studentized residuals of  $>3$  in  
601 absolute value.

602  
603  
604  
605



606  
607  
608  
609  
610  
611  
612  
613  
614  
615  
616  
617  
618  
619

**Fig. 3.** Comparison of innate immune gene repertoire and microbiome composition. **A.** Principle Coordinates Analysis (PCoA) of Weighted UniFrac Beta diversity distances for samples from all coral compartments, colored by genomic IL-1R copy number in the coral host. **B.** PCoA ordination of Weighted UniFrac distances for all compartments colored by genomic copy number for TLR genes. **C.** Phylogenetic independent contrasts regression of IL-1R copy number vs. Weighted UniFrac PC1 ( $R^2 = 0.917$ ,  $q_{\text{FDR}} = 0.00012$ ). **D.** Phylogenomorphospace of IL-1R copy number vs. Weighted UniFrac PC1. **E.** Phylogenetic independent contrasts regression of TLR copy number vs. Weighted UniFrac PC1 ( $R^2 = 0.774$ ,  $q_{\text{FDR}} = 0.0028$ ). **F.** Phylogenomorphospace of IL-1R copy number vs. Weighted UniFrac PC1. No correlations had outliers, as defined by studentized residuals of  $>3$  in absolute value.



620

621

**Fig. 4.** Heatmap showing microbial families significantly correlated with IL-1R and TLR copy numbers. Columns show correlations between the relative abundance of microbial families and IL-1R and TLR copy numbers in the mucus, tissue, and skeleton, respectively.

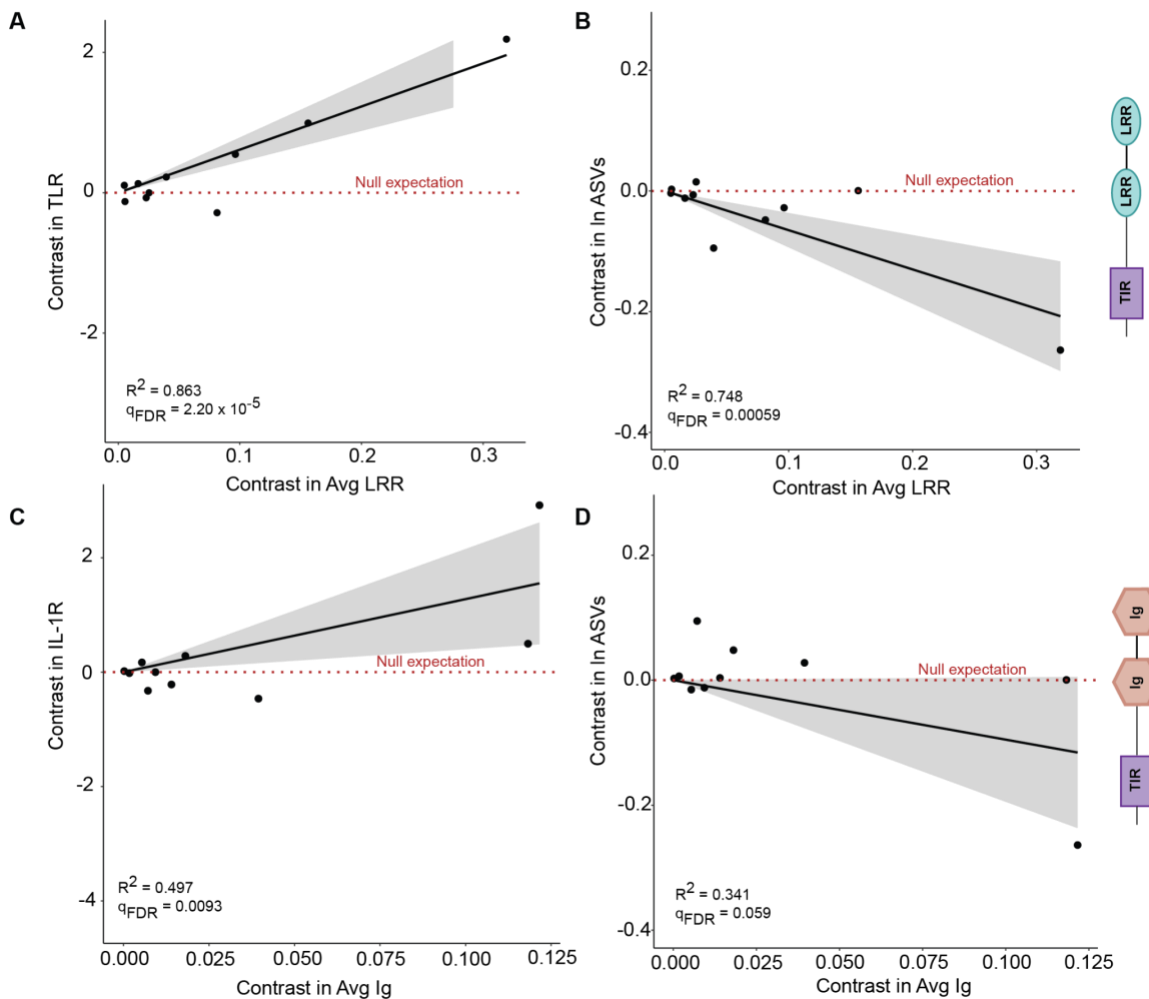
622

623

624

625

626



627

628

629

630

631

632

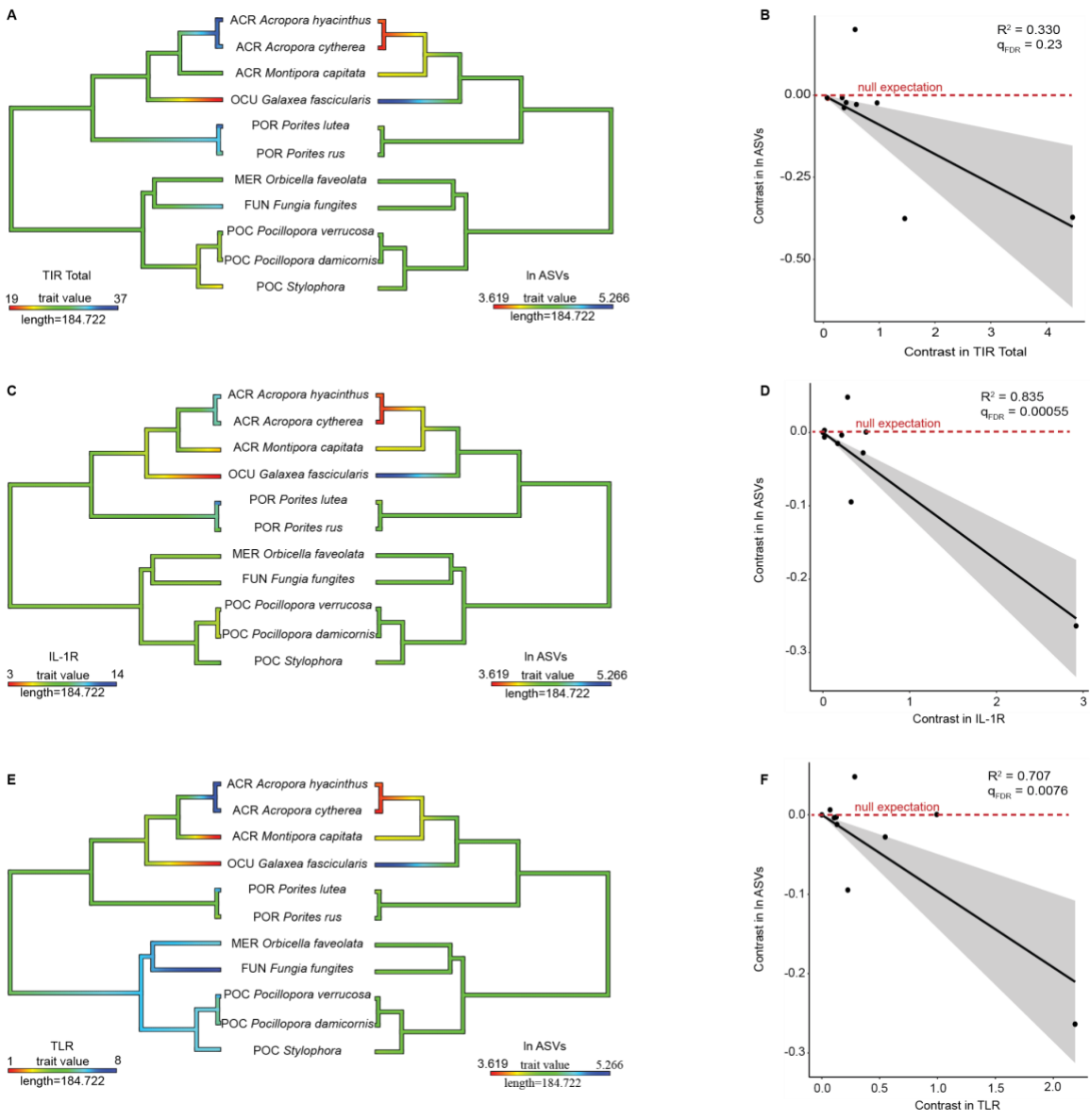
633

634

635

**Fig. 5.** Domain copy numbers influence microbiome richness. Phylogenetic contrasts comparing **A.** average LRR domain copies per TLR vs TLR domain copy number ( $R^2 = 0.863$ ,  $q_{FDR} = 2.20 \times 10^{-5}$ ), **B.** average LRR domain copies per TLR vs ln ASVs ( $R^2 = 0.748$ ,  $q_{FDR} = 0.00059$ ), **C.** average Ig domain copies per IL-1R vs IL-1R copy number ( $R^2 = 0.497$ ,  $q_{FDR} = 0.0093$ ), and **D.** average Ig domain copies per IL-1R vs ln ASVs per genome ( $R^2 = 0.341$ ,  $q_{FDR} = 0.059$ ).

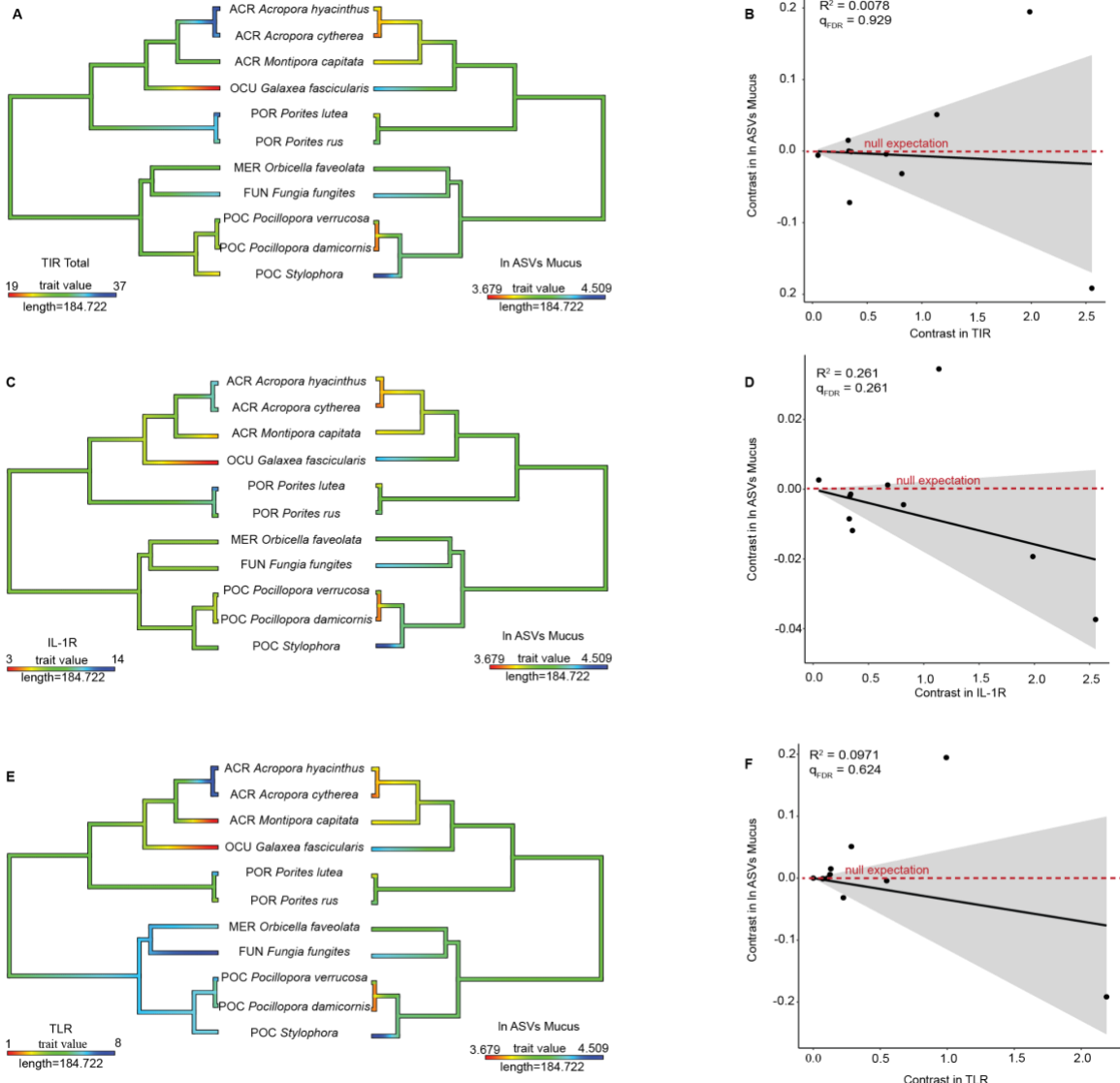
636  
637 **Supplementary Figures**  
638  
639 Supplementary Figures 1-4: Richness vs. gene copy number for 1) All compartments 2)  
640 mucus, 3 tissue, 4 skeleton  
641  
642 Supplementary Figures 5-8: Evenness vs. gene copy number for 1) All compartments 2)  
643 mucus, 3 tissue, 4 skeleton  
644  
645 Supplementary Figure 9: Comparison of domain copy number within genes and gene  
646 copies within genomes.  
647  
648 Supplementary Figure 10: Correlated responses of microbial families to TLR and IL-1R  
649 gene copy number  
650  
651 Supplementary Figures 11-16. Relative abundance of microbial classes in mucus 11,  
652 tissue 12 and skeleton 13 samples sorted by TLR copy number or IL-1R copy number  
653 (14,15,16).  
654  
655  
656  
657  
658  
659  
660  
661  
662



663  
664

**Fig. S1. Phylogenetic comparison of coral microbiome richness and innate immune repertoire for all compartments combined.** Rows show ancestral state reconstructions (left column) of innate immune gene copy number and microbiome richness, as well as phylogenetic independent contrast analysis for all predicted isoforms (right column) of **A,B** TIR-only genes ( $R^2 = 0.330$ ,  $q_{FDR} = 0.23$ ,  $p = 0.065$ ); **C,D** IL-1R genes ( $R^2 = 0.834$ ,  $q_{FDR} = 0.00055$ ,  $p = 5.14 \times 10^{-5}$ ); **E,F** TLR genes ( $R^2 = 0.707$ ,  $q_{FDR} = 0.0076$ ,  $p = 0.0012$ ) compared against log microbiome richness (ln ASVs). Shading in phylogenetic independent contrasts analysis indicates the 95% confidence interval of the mean.

672  
673



674  
675

676 **Fig. S2. Phylogenetic comparison of coral microbiome richness and innate immune**  
 677 **repertoire for the mucus compartment.** Rows show ancestral state reconstructions (left

678 column) of innate immune gene copy number and microbiome richness, as well as

679 phylogenetic independent contrast analysis for all predicted isoforms (right column) of

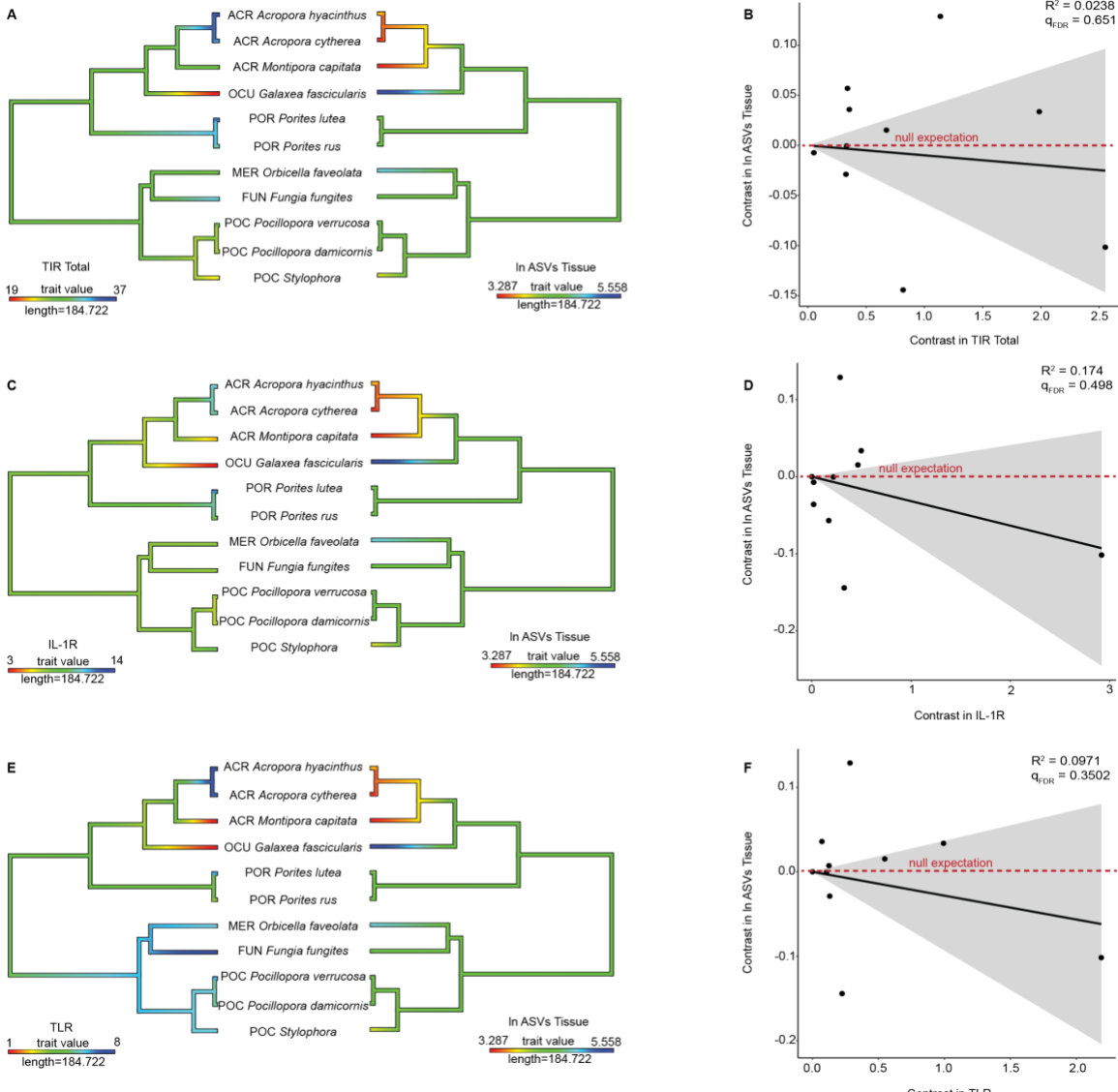
680 **A,B** TIR-only genes ( $R^2 = 0.0078$ ,  $q_{FDR} = 0.929$ ,  $p = 0.796$ ); **C,D** IL-1R genes ( $R^2 = 0.261$ ,

681  $q_{FDR} = 0.261$ ,  $p = 0.109$ ); **E,F** TLR genes ( $R^2 = 0.0971$ ,  $q_{FDR} = 0.624$ ,  $p = 0.351$ ) compared

682 against log microbiome richness (ln ASVs). Shading in phylogenetic independent

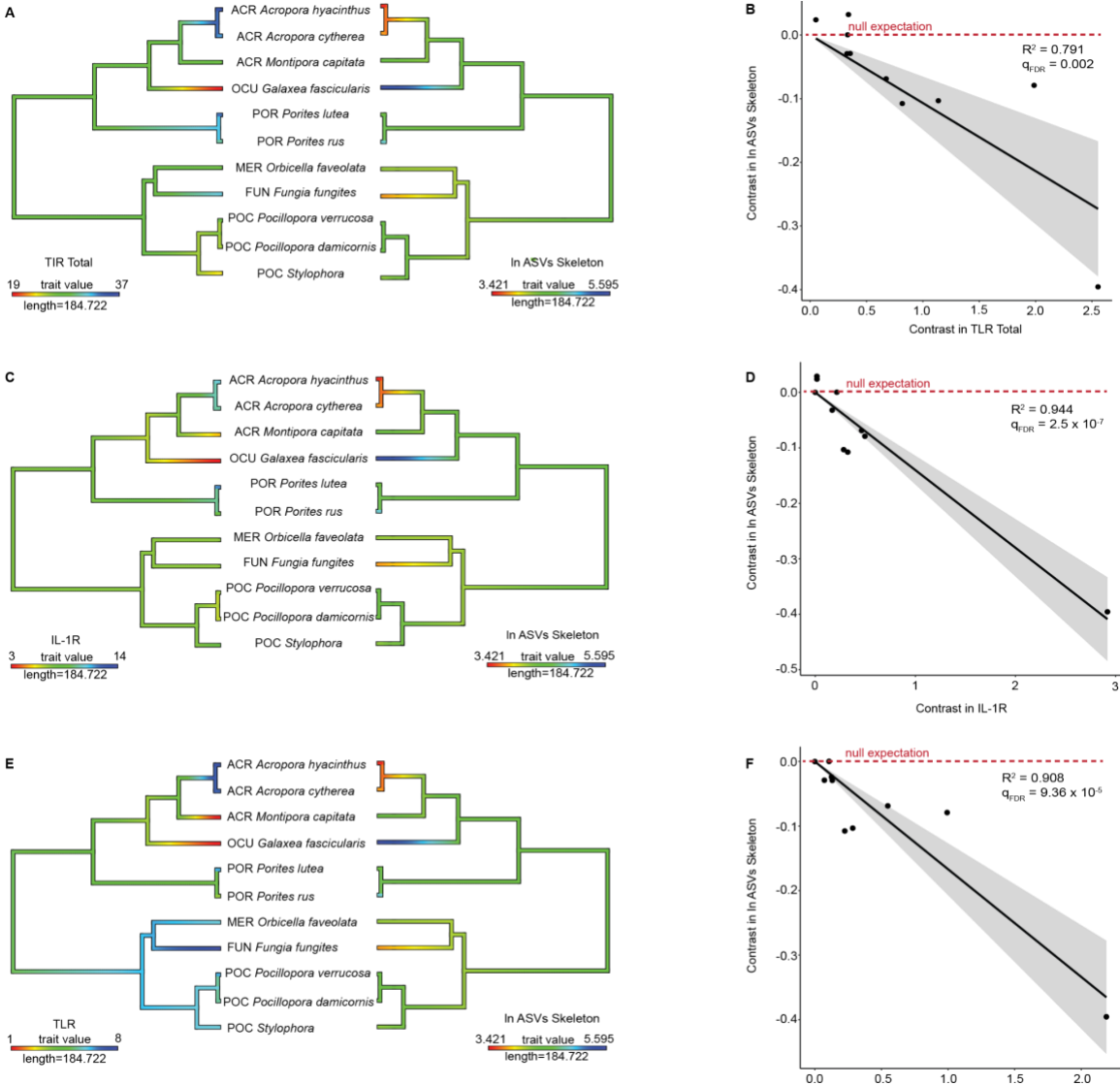
683 contrasts analysis indicates the 95% confidence interval of the mean.

684



685  
686  
687  
688  
689  
690  
691  
692  
693  
694  
695

**Fig. S3. Phylogenetic comparison of coral microbiome richness and innate immune repertoire for the tissue compartment.** Rows show ancestral state reconstructions (left column) of innate immune gene copy number and microbiome richness, as well as phylogenetic independent contrast analysis for all predicted isoforms (right column) of **A,B** TIR-only genes ( $R^2 = 0.0238$ ,  $q_{FDR}=0.929$ ,  $p = 0.651$ ); **C,D** IL-1R genes ( $R^2 = 0.174$ ,  $q_{FDR}=0.498$ ,  $p = 0.202$ ); **E,F** TLR genes ( $R^2 = 0.0974$ ,  $q_{FDR}=0.624$ ,  $p = 0.3502$ ) compared against log microbiome richness (ln ASVs). Shading in phylogenetic independent contrasts analysis indicates the 95% confidence interval of the mean.



696  
697

**Fig. S4. Phylogenetic comparison of coral microbiome richness and innate immune repertoire for the skeletal compartment.** Rows show ancestral state reconstructions (left column) of innate immune gene copy number and microbiome richness, as well as phylogenetic independent contrast analysis for all predicted isoforms (right column) of **A,B** TIR-only genes ( $R^2 = 0.791$ ,  $q_{FDR} = 0.002$ ,  $p = 0.000252$ ); **C,D** IL-1R genes ( $R^2 = 0.944$ ,  $q_{FDR} = 2.15 \times 10^{-5}$ ,  $p = 6.39 \times 10^{-7}$ ); **E,F** TLR genes ( $R^2 = 0.90798$ ,  $q_{FDR} = 9.36 \times 10^{-5}$ ,  $p = 5.85 \times 10^{-6}$ ) compared against log microbiome richness (ln ASVs). Shading in phylogenetic independent contrasts analysis indicates the 95% confidence interval of the mean.

708  
709  
710  
711  
712  
713  
714  
715  
716  
717  
718  
719

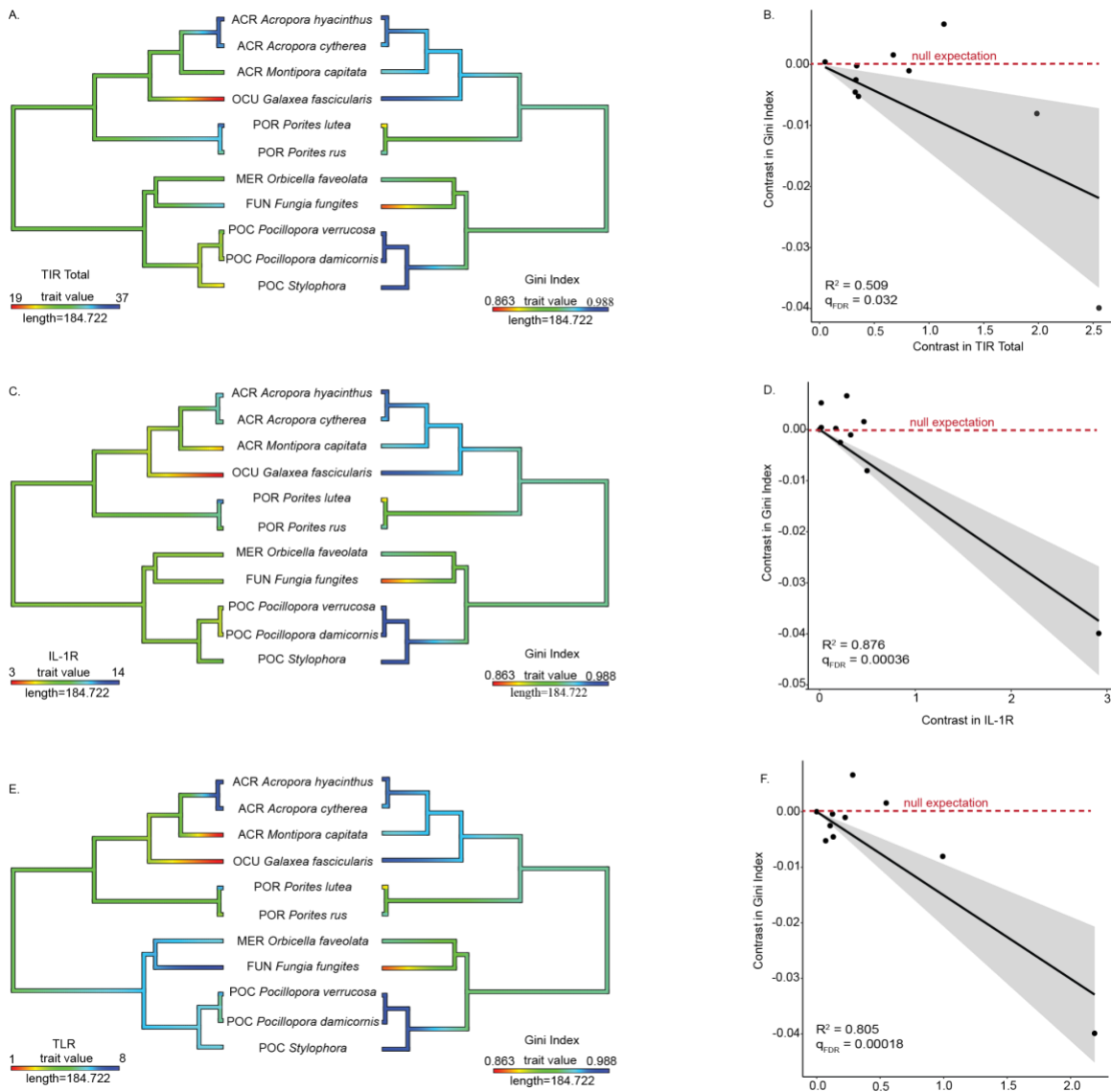


**Fig. S5. Phylogenetic comparison of coral microbiome evenness and innate immune repertoire in all compartments combined.** Rows show ancestral state reconstructions (left column) of innate immune gene copy number and microbiome evenness (Gini index), as well as phylogenetic independent contrast analysis for all predicted isoforms (right column) of **A,B** TIR-only genes ( $R^2 = 0.509$ ,  $q_{FDR} = 0.032$ ,  $p = 0.0083$ ); **C,D** IL-1R genes ( $R^2 = 0.876$ ,  $q_{FDR} = 0.00036$ ,  $p = 2.30 \times 10^{-5}$ ); **E,F** TLR genes ( $R^2 = 0.805$ ,  $q_{FDR} = 0.0014$ ,  $p = 0.00018$ ) compared against microbiome evenness (Gini index). Shading in phylogenetic independent contrasts analysis indicates the 95% confidence interval of the mean.

720  
721  
722  
723  
724  
725  
726  
727  
728  
729  
730

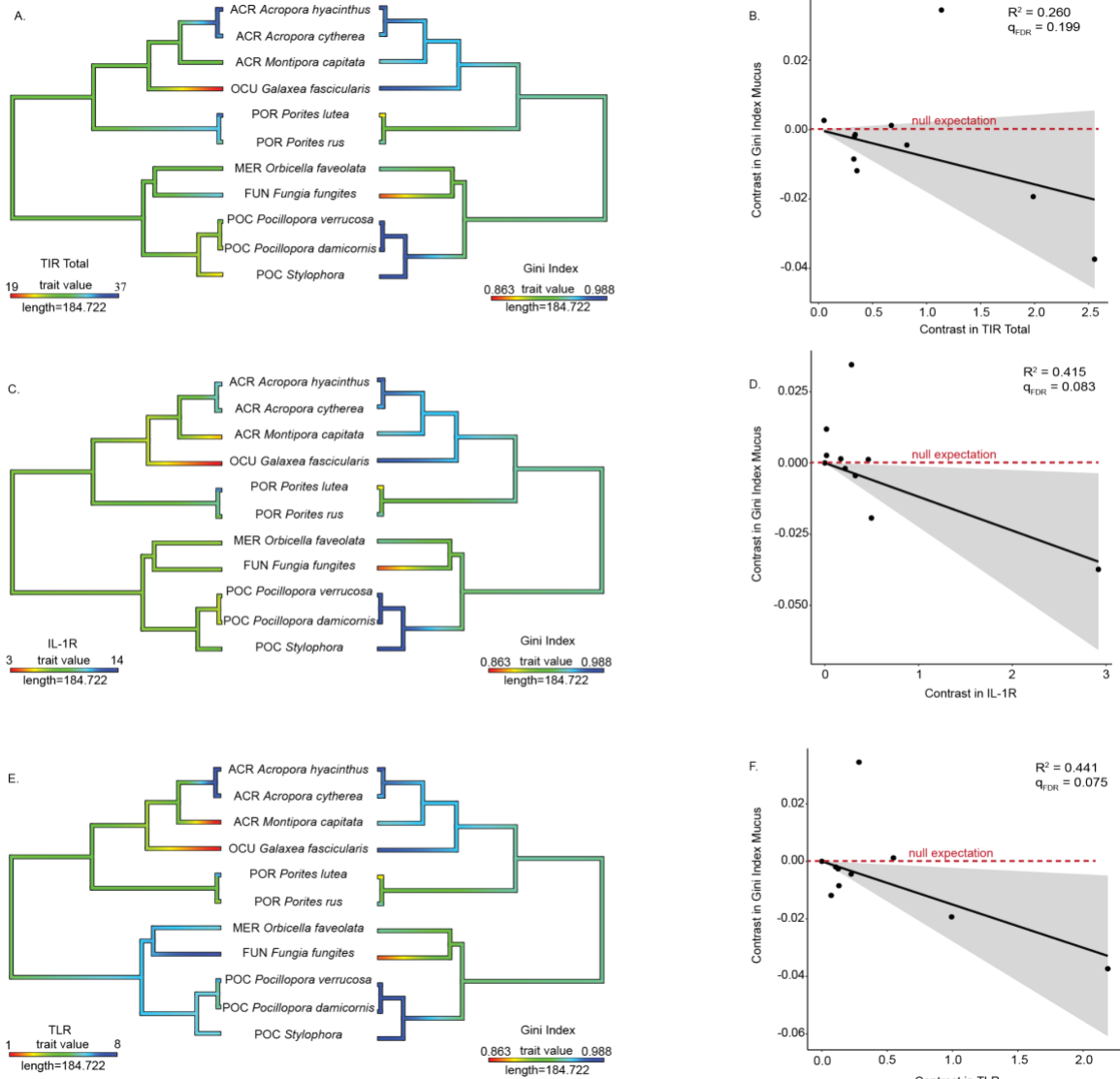


**Fig. S6. Phylogenetic comparison of coral microbiome evenness and innate immune repertoire in the mucus compartment.** Rows show ancestral state reconstructions (left column) of innate immune gene copy number and microbiome evenness (Gini index), as well as phylogenetic independent contrast analysis for all predicted isoforms (right column) of **A,B** TIR-only genes ( $R^2 = 0.260$ ,  $q_{FDR}=0.199$ ,  $p = 0.109$ ); **C,D** IL-1R genes ( $R^2 = 0.415$ ,  $q_{FDR}=0.083$ ,  $p = 0.0323$ ); **E,F** TLR genes ( $R^2 = 0.441$ ,  $q_{FDR}= 0.075$ ,  $p = 0.0258$ ) compared against microbiome evenness (Gini index). Shading in phylogenetic independent contrasts analysis indicates the 95% confidence interval of the mean.

731  
732  
733  
734  
735  
736  
737  
738  
739  
740  
741

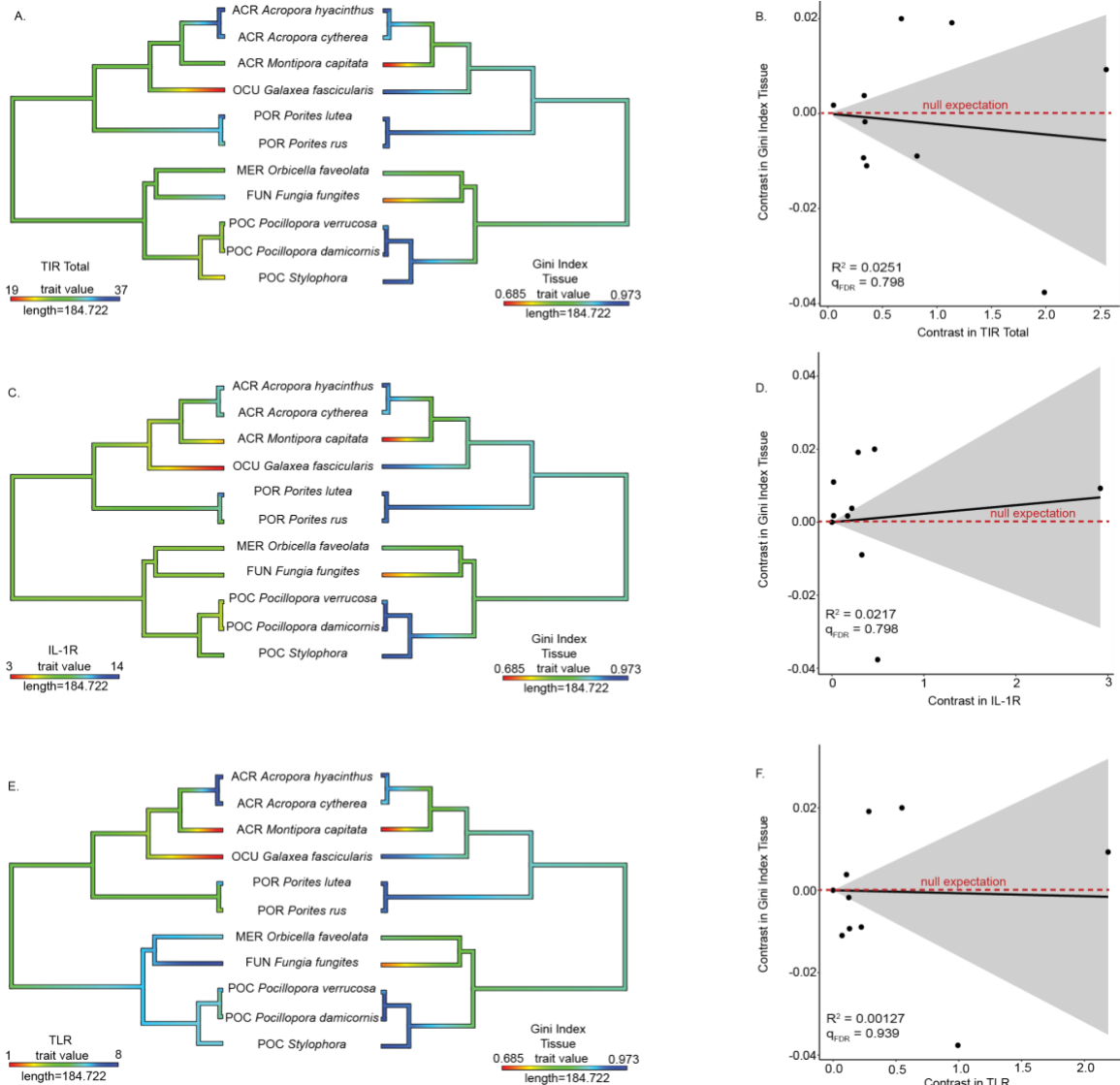


**Fig. S7. Phylogenetic comparison of coral microbiome evenness and innate immune repertoire in the tissue compartment.** Rows show ancestral state reconstructions (left column) of innate immune gene copy number and microbiome evenness (Gini index), as well as phylogenetic independent contrast analysis for all predicted isoforms (right column) of **A,B** TIR-only genes ( $R^2 = 0.0251$ ,  $q_{FDR} = 0.798$ ,  $p = 0.6421$ ); **C,D** IL-1R genes ( $R^2 = 0.0201$ ,  $q_{FDR} = 0.798$ ,  $p = 0.678$ ); **E,F** TLR genes ( $R^2 = 0.00127$ ,  $q_{FDR} = 0.939$ ,  $p = 0.917$ ) compared against microbiome evenness (Gini index). Shading in phylogenetic independent contrasts analysis indicates the 95% confidence interval of the mean.

742  
743  
744  
745  
746  
747  
748  
749  
750  
751  
752  
753

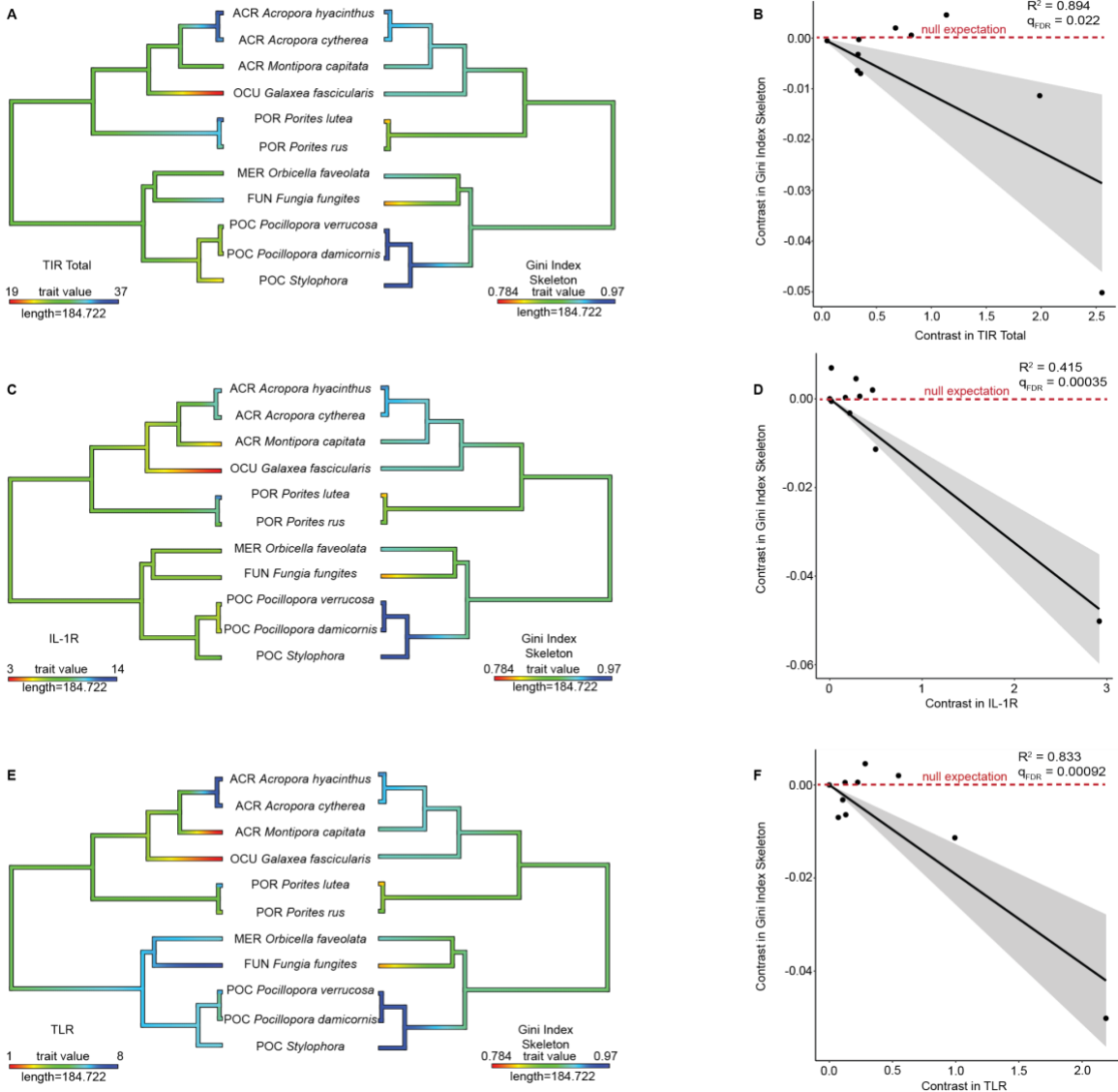
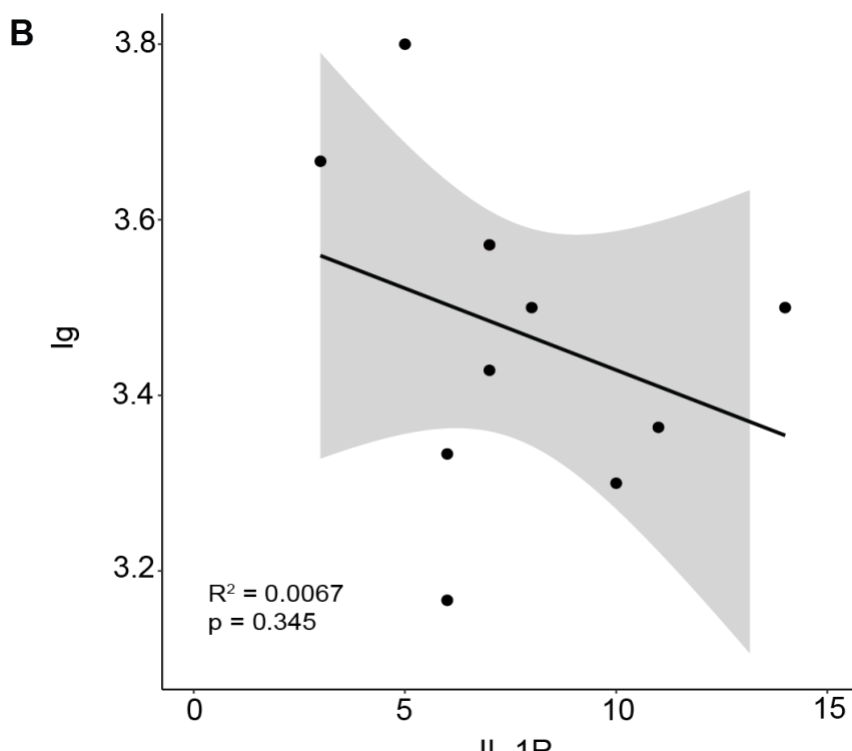
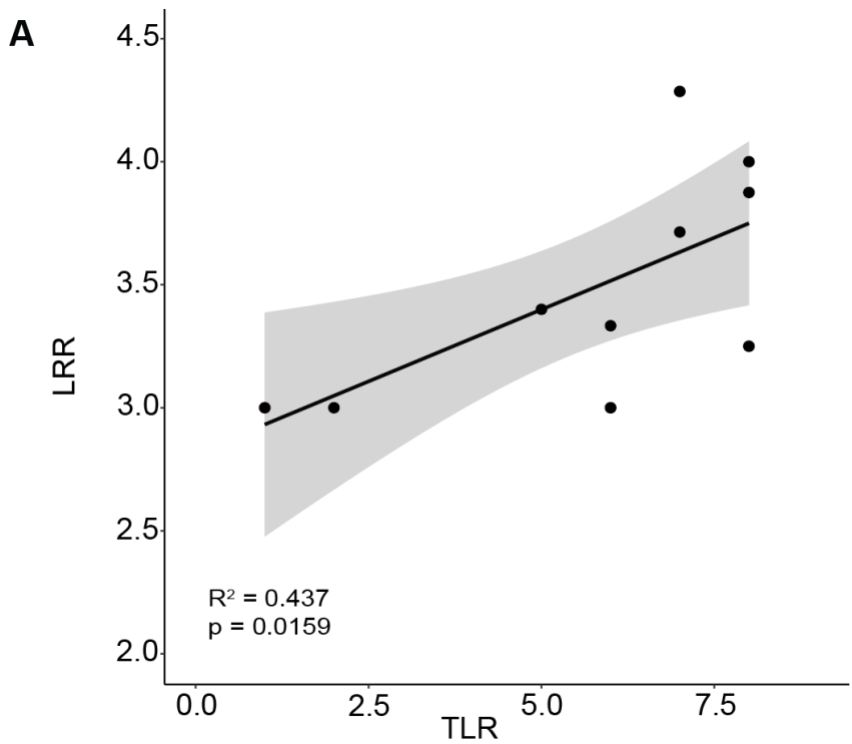


**Fig. S8. Phylogenetic comparison of coral microbiome evenness and innate immune repertoire in the skeleton compartment.** Rows show ancestral state reconstructions (left column) of innate immune gene copy number and microbiome evenness (Gini index), as well as phylogenetic independent contrast analysis for all predicted isoforms (right column) of **A,B** TIR-only genes ( $R^2 = 0.894$ ,  $q_{FDR}=0.022$ ,  $p = 1.12 \times 10^{-5}$ ); **C,D** IL-1R genes ( $R^2 = 0.415$ ,  $q_{FDR}=0.00035$ ,  $p = 0.0323$ ); **E,F** TLR genes ( $R^2 = 0.833$ ,  $q_{FDR}=0.00092$ ,  $p = 8.86 \times 10^{-5}$ ) compared against microbiome evenness (Gini index). Shading in phylogenetic independent contrasts analysis indicates the 95% confidence interval of the mean.

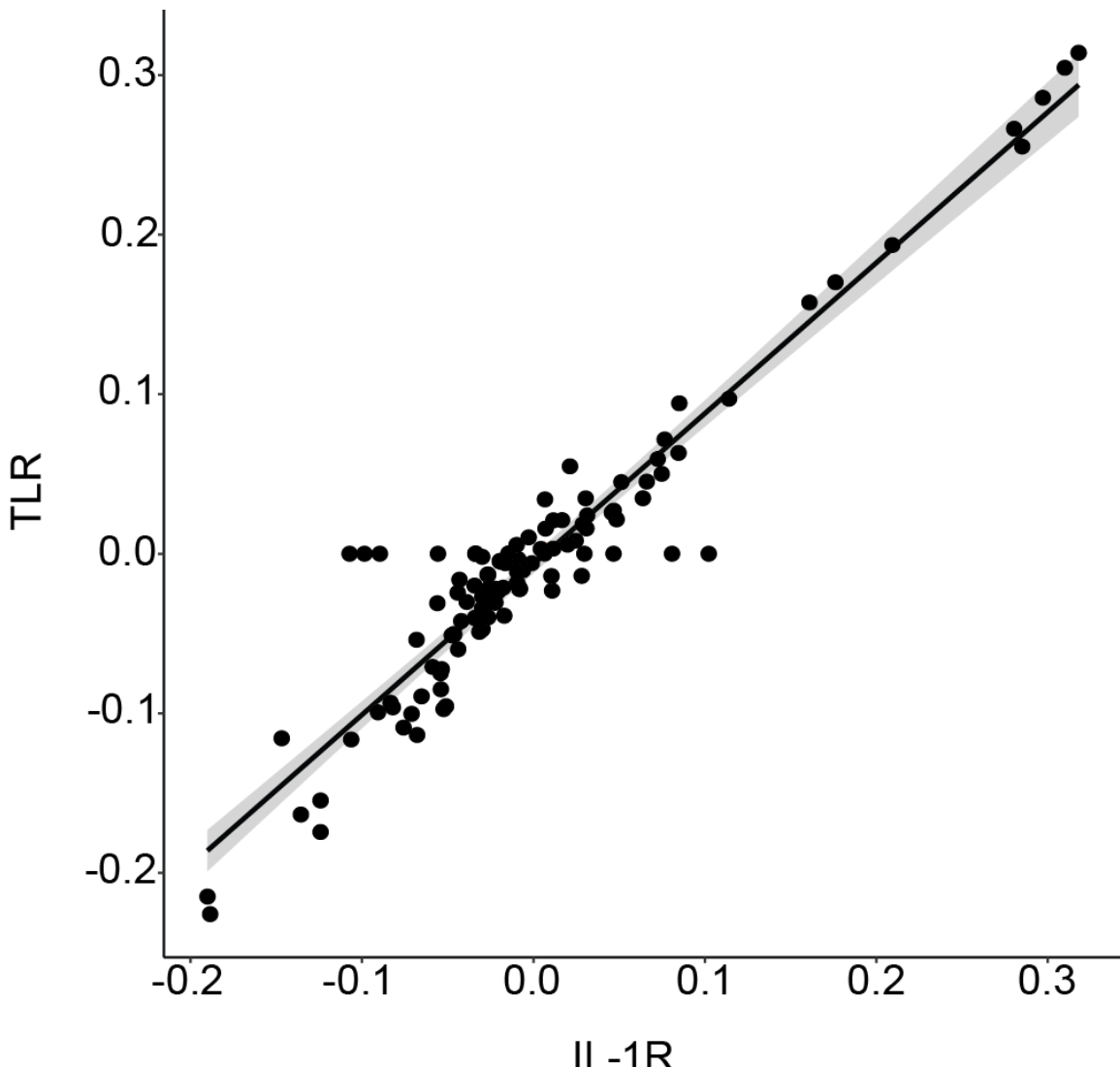


754

755

756 **Fig. S9. Comparison of domain copy number within genes and gene copies within**  
757 **genomes. A LRR domains vs TLR and B Ig vs IL-1R plots.**

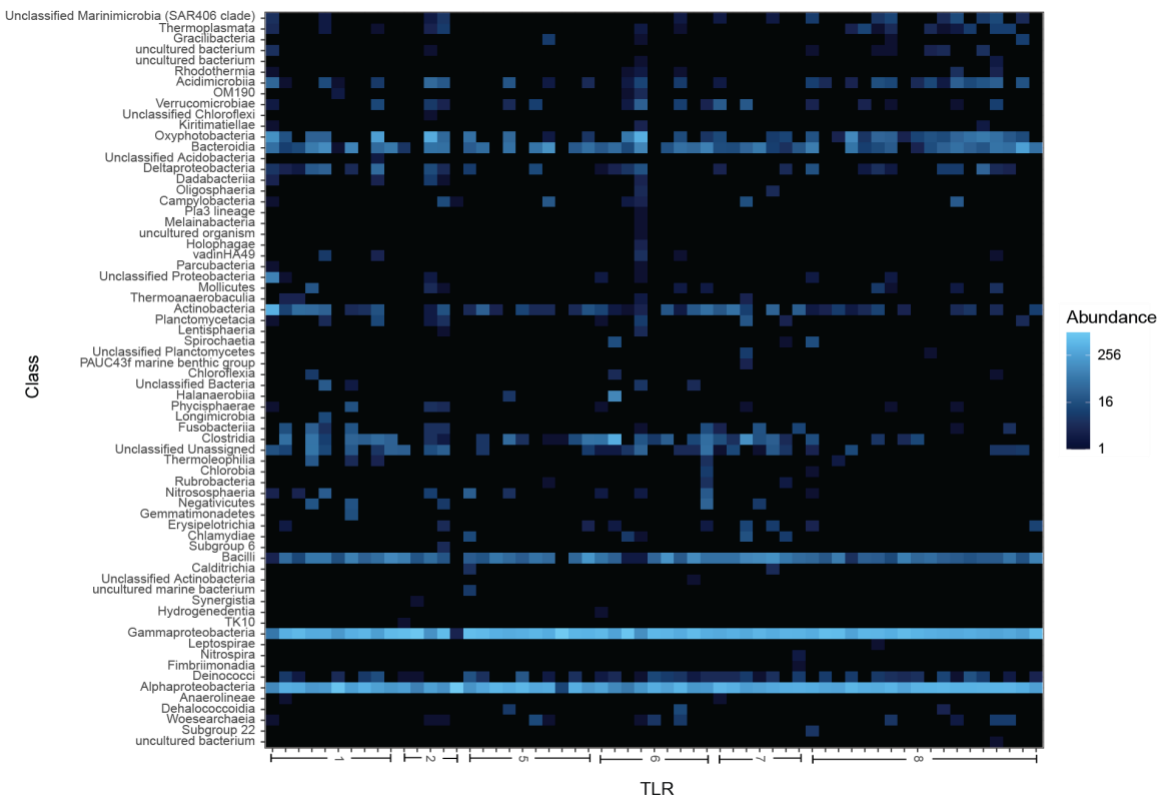
758



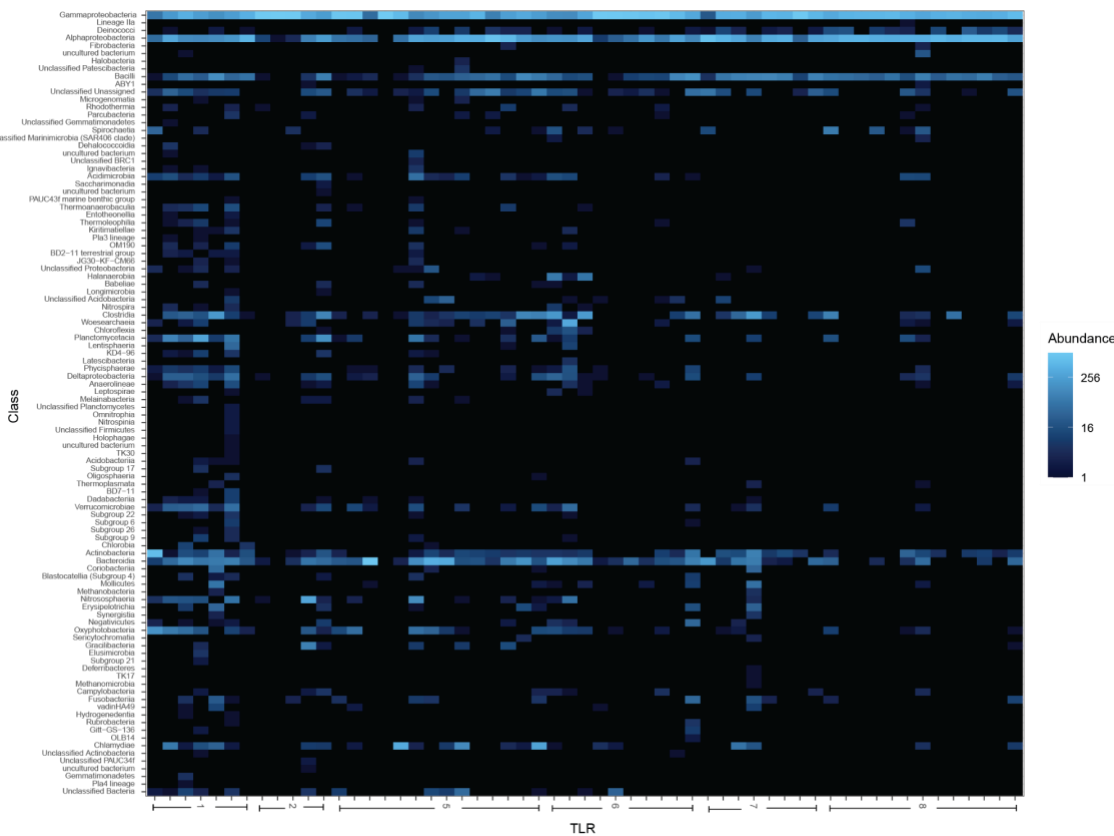
759

760

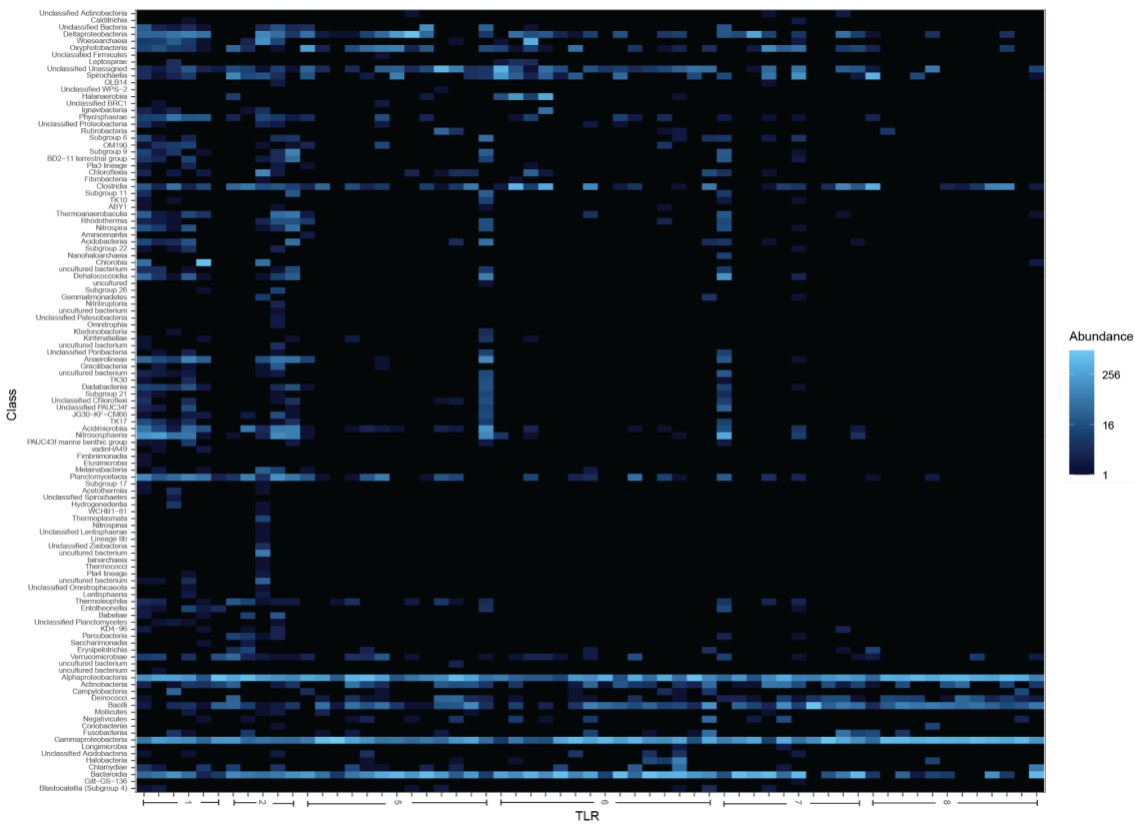
761 **Fig. S10. Correlated response of microbial families to IL-1R or TLR gene copy**  
762 **number over evolution.** Scatterplot shows contrasts in the correlation between microbial  
763 family relative abundance and IL-1R gene copy number (x-axis) and TLR gene copy  
764 number (y-axis). Each point represents one microbial family. Microbial families whose  
765 relative abundance is equally correlated with IL-1R and TLR gene copy number therefore  
766 fall near the diagonal.  
767



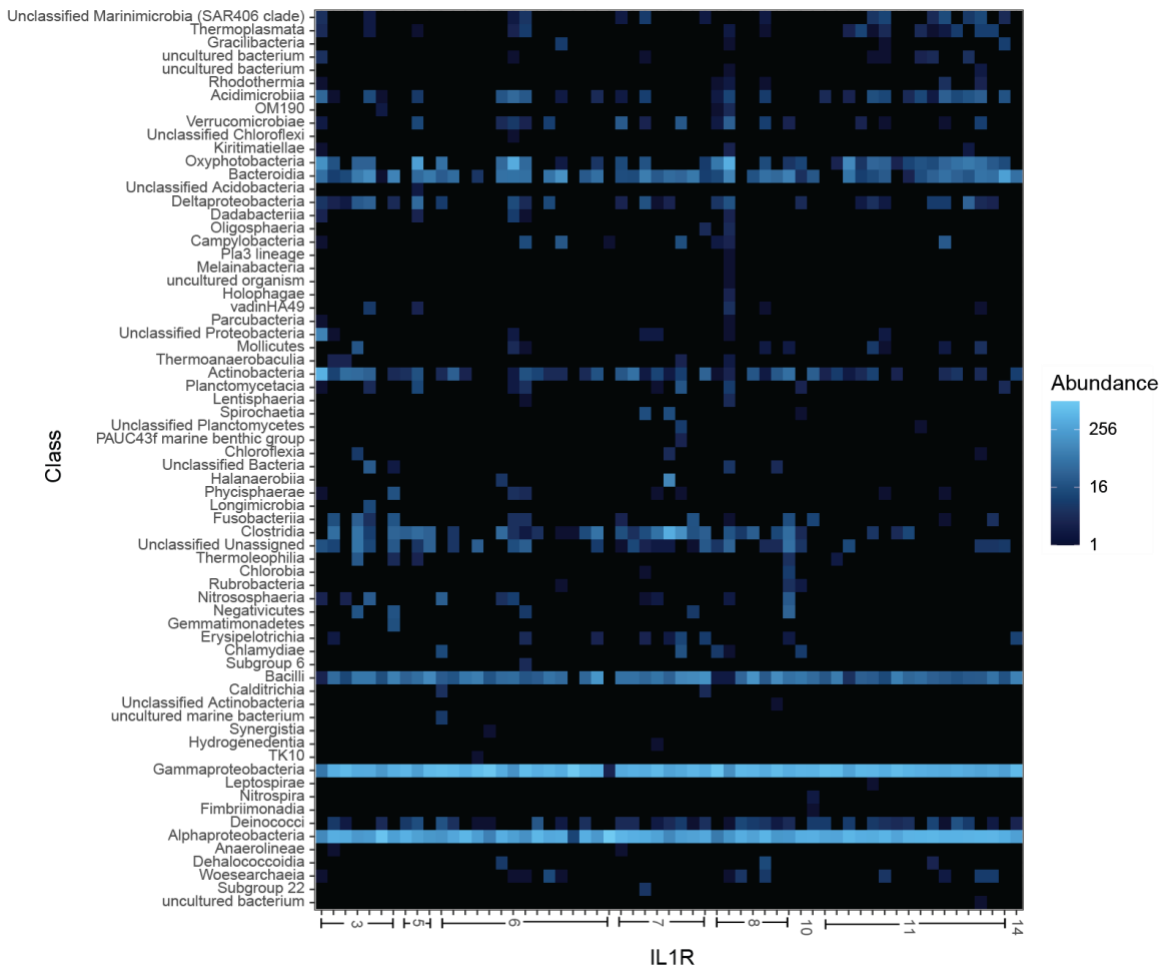
768  
769  
770 **Fig. S11. Heatmap of bacterial class abundance in mucus vs. TLR gene copy**  
771 **number.** Heatmap colors depict the relative abundance of bacterial classes in coral  
772 mucus (y-axis), in samples sorted by TLR gene copy number (x-axis). Colors reflect  
773 abundance per 1000 16S rRNA gene amplicon reads.  
774



775  
776  
777 **Fig. S12. Heatmap of bacterial class relative abundance in tissue vs. TLR gene copy**  
778 **number.** Heatmap colors depicts the relative abundance of bacterial classes in coral  
779 tissue (y-axis), in samples sorted by TLR gene copy number (x-axis). Colors reflect  
780 abundance per 1000 16S rRNA gene amplicon reads.  
781



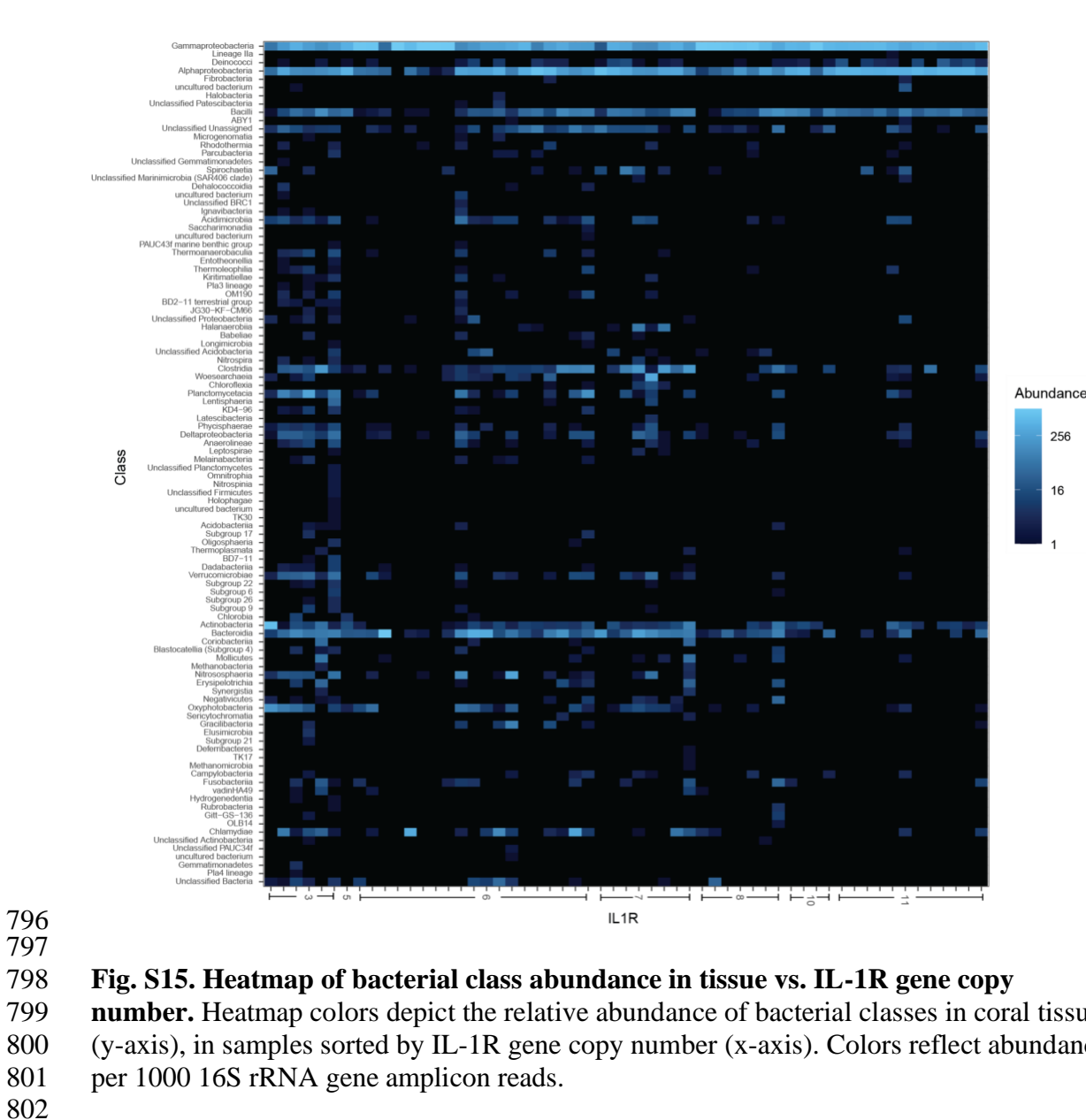
782  
783  
784 **Fig. S13. Heatmap of bacterial class relative abundance in skeleton vs. TLR gene**  
785 **copy number.** Heatmap colors depict the relative abundance of bacterial classes in coral  
786 skeleton (y-axis), in samples sorted by TLR gene copy number (x-axis). Colors reflect  
787 abundance per 1000 16S rRNA gene amplicon reads.  
788

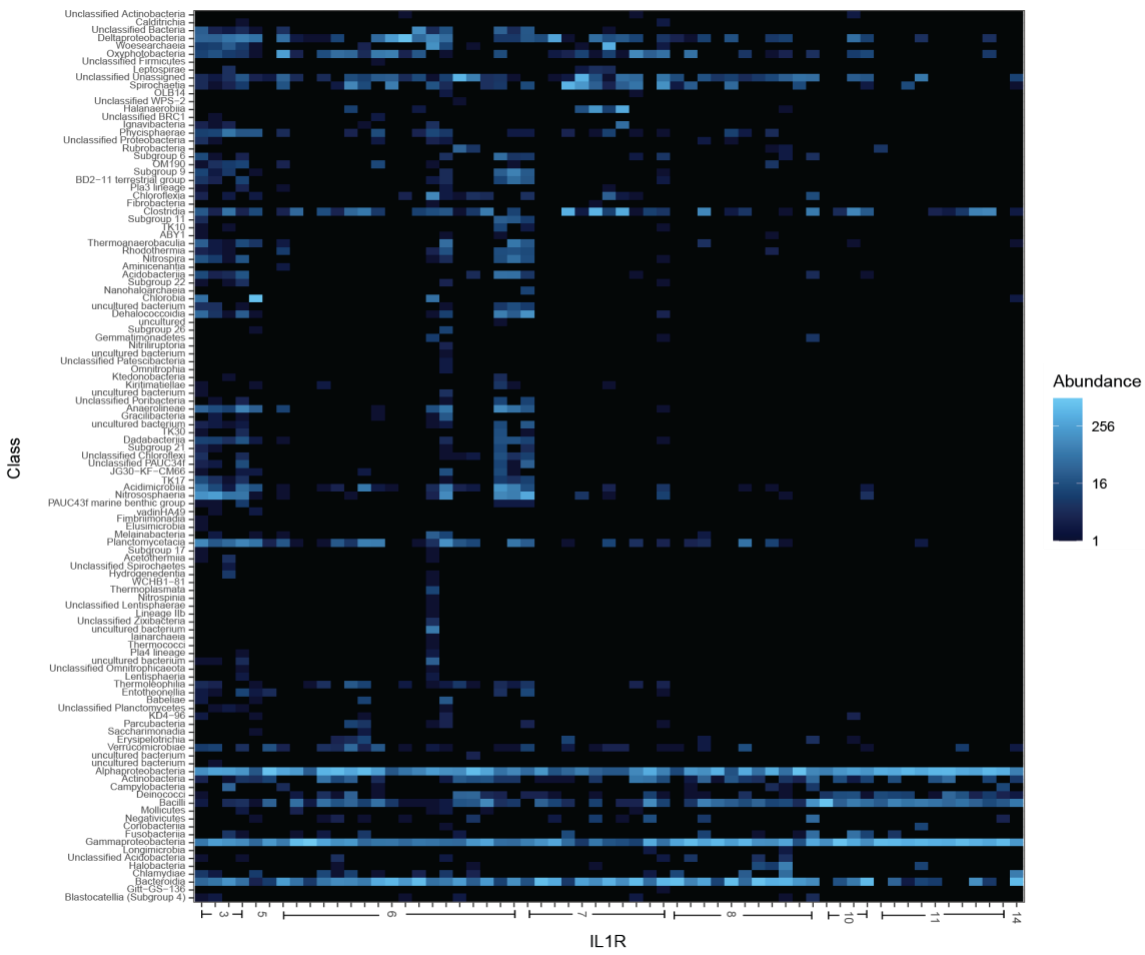


789  
790

**Fig. S14. Heatmap of bacterial class abundance in mucus vs. IL-1R gene copy number.** Heatmap colors depict the relative abundance of bacterial classes in coral mucus (y-axis), in samples sorted by IL-1R gene copy number (x-axis). Colors reflect abundance per 1000 16S rRNA gene amplicon reads.

791  
792  
793  
794  
795





803  
804

**Fig. S16. Heatmap of bacterial class abundance in skeleton vs. IL-1R gene copy number.** Heatmap colors depict the relative abundance of bacterial classes in coral skeleton (y-axis), in samples sorted by IL-1R gene copy number (x-axis). Colors reflect abundance per 1000 16S rRNA gene amplicon reads.

809  
810  
811  
812  
813  
814  
815  
816  
817  
818  
819  
820  
821  
822

823 **Supplementary Data Tables**  
824

825 **Supplementary Table 1.** Sample and Genomic metadata. (A) Genomes used in the  
826 analysis (B) Per sample metadata for the GCMP data (C) Mapping file for the GCMP  
827 data.

828  
829 **Supplementary Table 2.** Annotations of TIR-domain containing gene families in coral  
830 genomes for (A) Total number of IL-1R and TLR genes, (B) Domain make up of IL-1R  
831 genes, (C) Domain make up of TLR genes.

832  
833 **Supplementary Table 3.** Quality control information for the sequencing depth of  
834 microbiome samples in the dataset.

835  
836 **Supplementary Table 4.** Distribution of TIR, LRR, and Ig domains across unique  
837 predicted protein isoforms in sequenced coral genomes.

838  
839 **Supplementary Table 5.** Microbiome (A) richness and (B) evenness across samples in  
840 the analysis.

841  
842 **Supplementary Table 6.** Phylogenetic comparison of IL-1R and TLR gene family copy  
843 number vs. microbiome alpha diversity in (A) All Samples (B) Mucus (C) Tissue, (D)  
844 Skeleton.

845  
846 **Supplementary Table 7.** Trait table of the genomic and microbiome traits of coral  
847 species in the analysis.

848  
849 **Supplementary Table 8.** Phylogenetic comparison of TIR LRR and Ig domains vs.  
850 microbiome alpha diversity in A) All Samples B) Mucus c) Tissue, d) Skeleton.

851  
852 **Supplementary Table 9.** Phylogenetic comparison of IL-1R and TLR gene family copy  
853 number vs. PC axes from beta-diversity PCoA analysis in (A) All Samples (B) Mucus  
854 (C) Tissue, (D) Skeleton.

855  
856 **Supplementary Table 10.** ANCOMBC comparison of relative abundance of microbial  
857 taxa vs. IL-1R and TLR gene family copy number in (A) All Samples (B) Mucus (C)  
858 Tissue, (D) Skeleton.

859  
860 **Supplementary Table 11.** Phylogenetic comparison of TIR LRR and Ig domains vs.  
861 microbiome PC axes from beta-diversity PCoA analysis in (A) All Samples (B) Mucus  
862 (C) Tissue, (D) Skeleton.

863  
864  
865  
866  
867  
868  
869

870

871 **References**

- 872 1. Hoeksema, B. W. & Cairns, S. *World List of Scleractinia*.  
873 <https://www.marinespecies.org/scleractinia>.
- 874 2. Rohwer, F., Seguritan, V., Azam, F. & Knowlton, N. Diversity and distribution of  
875 coral-associated bacteria. *Mar. Ecol. Prog. Ser.* **243**, 1–10 (2002).
- 876 3. Pollock, F. J. *et al.* Coral-associated bacteria demonstrate phylosymbiosis and  
877 cophylogeny. *Nat. Commun.* **9**, 4921 (2018).
- 878 4. Ricci, F. *et al.* Host Traits and Phylogeny Contribute to Shaping Coral-Bacterial  
879 Symbioses. *Msystems* **7**, e00044-22 (2022).
- 880 5. Hernandez-Agreda, A., Leggat, W., Bongaerts, P., Herrera, C. & Ainsworth, T. D.  
881 Rethinking the coral microbiome: simplicity exists within a diverse microbial biosphere.  
882 *MBio* **9**, e00812-18 (2018).
- 883 6. Littman, R. A., Willis, B. L., Pfeffer, C. & Bourne, D. G. Diversities of coral-  
884 associated bacteria differ with location, but not species, for three acroporid corals on the  
885 Great Barrier Reef. *FEMS Microbiol. Ecol.* **68**, 152–163 (2009).
- 886 7. Rodriguez-Lanetty, M., Granados-Cifuentes, C., Barberan, A., Bellantuono, A. J.  
887 & Bastidas, C. Ecological Inferences from a deep screening of the Complex Bacterial C  
888 onsortia associated with the coral, *Porites astreoides*. *Mol. Ecol.* **22**, 4349–4362 (2013).
- 889 8. Pantos, O., Bongaerts, P., Dennis, P. G., Tyson, G. W. & Hoegh-Guldberg, O.  
890 Habitat-specific environmental conditions primarily control the microbiomes of the coral  
891 *Seriatopora hystrix*. *ISME J.* **9**, 1916–1927 (2015).
- 892 9. Dunphy, C. M., Gouhier, T. C., Chu, N. D. & Vollmer, S. V. Structure and  
893 stability of the coral microbiome in space and time. *Sci. Rep.* **9**, 1–13 (2019).
- 894 10. Wang, L. *et al.* Corals and their microbiomes are differentially affected by  
895 exposure to elevated nutrients and a natural thermal anomaly. *Front. Mar. Sci.* **5**, 101  
896 (2018).
- 897 11. Pootakham, W. *et al.* Heat-induced shift in coral microbiome reveals several  
898 members of the Rhodobacteraceae family as indicator species for thermal stress in *Porites*  
899 *lutea*. *MicrobiologyOpen* **8**, e935 (2019).
- 900 12. Ricci, F. *et al.* Beneath the surface: community assembly and functions of the  
901 coral skeleton microbiome. *Microbiome* **7**, 1–10 (2019).

- 914 13. Kusdianto, H. *et al.* Microbiomes of Healthy and Bleached Corals During a 2016  
915 Thermal Bleaching Event in the Upper Gulf of Thailand. *Front. Mar. Sci.* **8**, 643962  
916 (2021).
- 917 14. Marchioro, G. M. *et al.* Microbiome dynamics in the tissue and mucus of  
918 acroporid corals differ in relation to host and environmental parameters. *PeerJ* **8**, e9644  
919 (2020).
- 920 15. Fifer, J. E. *et al.* Microbiome structuring within a coral colony and along a  
921 sedimentation gradient. *Cell. Stress Response Physiol. Adapt. Corals Subj. Environ.*  
922 *Stress. Pollut.* (2022).
- 923 16. Zaneveld, J. R. *et al.* Overfishing and nutrient pollution interact with temperature  
924 to disrupt coral reefs down to microbial scales. *Nat. Commun.* **7**, 1–12 (2016).
- 925 17. Corinaldesi, C. *et al.* Multiple impacts of microplastics can threaten marine  
926 habitat-forming species. *Commun. Biol.* **4**, 1–13 (2021).
- 927 18. Pratte, Z. A., Longo, G. O., Burns, A. S., Hay, M. E. & Stewart, F. J. Contact with  
928 turf algae alters the coral microbiome: contact versus systemic impacts. *Coral Reefs* **37**,  
929 1–13 (2018).
- 930 19. Briggs, A. A., Brown, A. L. & Osenberg, C. W. Local versus site-level effects of  
931 algae on coral microbial communities. *R. Soc. Open Sci.* **8**, 210035 (2021).
- 932 20. Miller, N., Maneval, P., Manfrino, C., Frazer, T. K. & Meyer, J. L. Spatial  
933 distribution of microbial communities among colonies and genotypes in nursery-reared  
934 *Acropora cervicornis*. *PeerJ* **8**, e9635 (2020).
- 935 21. Palacio-Castro, A. M., Rosales, S. M., Dennison, C. E. & Baker, A. C.  
936 Microbiome signatures in *Acropora cervicornis* are associated with genotypic resistance  
937 to elevated nutrients and heat stress. *Coral Reefs* **41**, 1389–1403 (2022).
- 938 22. Rosales, S. M. *et al.* Microbiome differences in disease-resistant vs. susceptible  
939 *Acropora* corals subjected to disease challenge assays. *Sci. Rep.* **9**, 18279 (2019).
- 940 23. Rosado, P. M. *et al.* Marine probiotics: increasing coral resistance to bleaching  
941 through microbiome manipulation. *ISME J.* **13**, 921–936 (2019).
- 942 24. Ley, R. E. *et al.* Evolution of mammals and their gut microbes. *science* **320**,  
943 1647–1651 (2008).
- 944 25. Bodawatta, K. H. *et al.* Species-specific but not phylosymbiotic gut microbiomes  
945 of New Guinean passerine birds are shaped by diet and flight-associated gut  
946 modifications. *Proc. R. Soc. B* **288**, 20210446 (2021).
- 947 950 953 956 959

- 960 26. Poole, A. Z. & Weis, V. M. TIR-domain-containing protein repertoire of nine  
961 anthozoan species reveals coral-specific expansions and uncharacterized proteins. *Dev.*  
962 *Comp. Immunol.* **46**, 480–488 (2014).
- 963
- 964 27. Medzhitov, R. & Janeway, C. A. Innate immunity: the virtues of a nonclonal  
965 system of recognition. *Cell* **91**, 295–298 (1997).
- 966
- 967 28. Thompson, L. R. *et al.* A communal catalogue reveals Earth's multiscale  
968 microbial diversity. *Nature* **551**, 457–463 (2017).
- 969
- 970 29. Parada, A. E., Needham, D. M. & Fuhrman, J. A. Every base matters: assessing  
971 small subunit rRNA primers for marine microbiomes with mock communities, time series  
972 and global field samples. *Environ. Microbiol.* **18**, 1403–1414 (2016).
- 973
- 974 30. Apprill, A., McNally, S., Parsons, R. & Weber, L. Minor revision to V4 region  
975 SSU rRNA 806R gene primer greatly increases detection of SAR11 bacterioplankton.  
976 *Aquat. Microb. Ecol.* **75**, 129–137 (2015).
- 977
- 978 31. Caporaso, J. G. EMP 16S Illumina Amplicon Protocol. (2018)  
979 doi:10.17504/protocols.io.nuudeww.
- 980
- 981 32. Gonzalez, A. *et al.* Qiita: rapid, web-enabled microbiome meta-analysis. *Nat.*  
982 *Methods* **15**, 796–798 (2018).
- 983
- 984 33. Caporaso, J. G. *et al.* QIIME allows analysis of high-throughput community  
985 sequencing data. *Nat. Methods* **7**, 335–336 (2010).
- 986
- 987 34. Amir, A. *et al.* Deblur Rapidly Resolves Single-Nucleotide Community Sequence  
988 Patterns. *mSystems* **2**, e00191-16 (2017).
- 989
- 990 35. Bolyen, E. *et al.* QIIME 2: Reproducible, interactive, scalable, and extensible  
991 microbiome data science. <https://peerj.com/preprints/27295> (2018)  
992 doi:10.7287/peerj.preprints.27295v2.
- 993
- 994 36. Rognes, T., Flouri, T., Nichols, B., Quince, C. & Mahé, F. VSEARCH: a versatile  
995 open source tool for metagenomics. *PeerJ* **4**, e2584 (2016).
- 996
- 997 37. Quast, C. *et al.* The SILVA ribosomal RNA gene database project: improved data  
998 processing and web-based tools. *Nucleic Acids Res.* **41**, D590–D596 (2013).
- 999
- 1000 38. Bengtsson-Palme, J. *et al.* METAXA2: improved identification and taxonomic  
1001 classification of small and large subunit rRNA in metagenomic data. *Mol. Ecol. Resour.*  
1002 **15**, 1403–1414 (2015).
- 1003
- 1004 39. Sonett, D., Brown, T., Bengtsson-Palme, J., Padilla-Gamiño, J. L. & Zaneveld, J.  
1005 R. The Organelle in the Room: Under-annotated Mitochondrial Reads Bias Coral

- 1006 Microbiome Analysis. <http://biorxiv.org/lookup/doi/10.1101/2021.02.23.431501> (2021)  
1007 doi:10.1101/2021.02.23.431501.
- 1008
- 1009 40. Janssen, S. *et al.* Phylogenetic Placement of Exact Amplicon Sequences Improves  
1010 Associations with Clinical Information. *mSystems* **3**, (2018).
- 1011
- 1012 41. Lin, H. & Peddada, S. D. Analysis of compositions of microbiomes with bias  
1013 correction. *Nat. Commun.* **11**, 1–11 (2020).
- 1014
- 1015 42. Emery, M. A., Dimos, B. A. & Mydlarz, L. D. Cnidarian pattern recognition  
1016 receptor repertoires reflect both phylogeny and life history traits. *Front. Immunol.* **12**,  
1017 689463 (2021).
- 1018
- 1019 43. Mazel, F. *et al.* Is host filtering the main driver of phylosymbiosis across the tree  
1020 of life? *Msystems* **3**, e00097-18 (2018).
- 1021
- 1022 44. Brooks, A. W., Kohl, K. D., Brucker, R. M., van Opstal, E. J. & Bordenstein, S.  
1023 R. Phylosymbiosis: Relationships and Functional Effects of Microbial Communities  
1024 across Host Evolutionary History. *PLOS Biol.* **14**, e2000225 (2016).
- 1025
- 1026 45. O'Brien, P. A. *et al.* Diverse coral reef invertebrates exhibit patterns of  
1027 phylosymbiosis. *ISME J.* **14**, 2211–2222 (2020).
- 1028
- 1029 46. Delsuc, F. *et al.* Convergence of gut microbiomes in myrmecophagous mammals.  
1030 *Mol. Ecol.* **23**, 1301–1317 (2014).
- 1031
- 1032 47. Song, S. J. *et al.* Is there convergence of gut microbes in blood-feeding  
1033 vertebrates? *Philos. Trans. R. Soc. B Biol. Sci.* **374**, 20180249 (2019).
- 1034
- 1035 48. Song, S. J. *et al.* Comparative Analyses of Vertebrate Gut Microbiomes Reveal  
1036 Convergence between Birds and Bats. *mbio* **11**, e02901-19 (2020).
- 1037
- 1038 49. Palmer, C. V. *et al.* Patterns of coral ecological immunology: variation in the  
1039 responses of Caribbean corals to elevated temperature and a pathogen elicitor. *J. Exp.*  
1040 *Biol.* **214**, 4240–4249 (2011).
- 1041
- 1042 50. Palmer, C., Bythell, J. & Willis, B. Enzyme activity demonstrates multiple  
1043 pathways of innate immunity in Indo-Pacific anthozoans. *Proc. R. Soc. B Biol. Sci.* **279**,  
1044 3879–3887 (2012).
- 1045
- 1046 51. Brown, T., Sonett, D., Zaneveld, J. R. & Padilla-Gamiño, J. L. Characterization of  
1047 the microbiome and immune response in corals with chronic Montipora white syndrome.  
1048 *Mol. Ecol.* **30**, 2591–2606 (2021).
- 1049
- 1050 52. Thaiss, C. A., Levy, M., Suez, J. & Elinav, E. The interplay between the innate  
1051 immune system and the microbiota. *Curr. Opin. Immunol.* **26**, 41–48 (2014).

- 1052  
1053 53. Fonseca, J. P., Lakshmanan, V., Boschiero, C. & Mysore, K. S. The Pattern  
1054 Recognition Receptor FLS2 Can Shape the Arabidopsis Rhizosphere Microbiome  $\beta$ -  
1055 Diversity but Not EFR1 and CERK1. *Plants* **11**, 1323 (2022).
- 1056  
1057 54. Axworthy, J. B. *et al.* Shotgun Proteomics Identifies Active Metabolic Pathways  
1058 in Bleached Coral Tissue and Intraskelatal Compartments. *Front. Mar. Sci.* (2022).
- 1059  
1060 55. Levy, S. & Mass, T. The Skeleton and Biomineralization Mechanism as Part of  
1061 the Innate Immune System of Stony Corals. *Front. Immunol.* **13**, (2022).
- 1062  
1063 56. Vega Thurber, R. *et al.* Deciphering coral disease dynamics: integrating host,  
1064 microbiome, and the changing environment. *Front. Ecol. Evol.* **8**, 575927 (2020).
- 1065  
1066 57. Elton, C. S. *The Ecology of Invasions by Animals and Plants*. (Springer Nature,  
1067 2020).
- 1068  
1069 58. Marraffini, M. L. & Geller, J. B. Species richness and interacting factors control  
1070 invasibility of a marine community. *Proc. R. Soc. B Biol. Sci.* **282**, 20150439 (2015).
- 1071  
1072 59. Sommer, F. *et al.* Microbiomarkers in inflammatory bowel diseases: caveats come  
1073 with caviar. *Gut* **66**, 1734–1738 (2017).
- 1074  
1075 60. Sommer, F., Anderson, J. M., Bharti, R., Raes, J. & Rosenstiel, P. The resilience  
1076 of the intestinal microbiota influences health and disease. *Nat. Rev. Microbiol.* **15**, 630–  
1077 638 (2017).
- 1078  
1079 61. Palmer, C. V. Immunity and the coral crisis. *Commun. Biol.* **1**, 91 (2018).
- 1080  
1081 62. Feng, G., Sun, W., Zhang, F., Karthik, L. & Li, Z. Inhabitancy of active  
1082 Nitrosopumilus-like ammonia-oxidizing archaea and Nitrospira nitrite-oxidizing bacteria  
1083 in the sponge Theonella swinhonis. *Sci. Rep.* **6**, 1–11 (2016).
- 1084  
1085 63. Kim, S.-H., Kim, J.-H., Park, M.-A., Hwang, S. D. & Kang, J.-C. The toxic  
1086 effects of ammonia exposure on antioxidant and immune responses in Rockfish, *Sebastes*  
1087 *schlegelii* during thermal stress. *Environ. Toxicol. Pharmacol.* **40**, 954–959 (2015).
- 1088  
1089 64. Kvennafors, E., Sampayo, E., Ridgway, T., Barnes, A. & Hoegh-Guldberg, O.  
1090 Bacterial Communities of Two Ubiquitous Great Barrier Reef Corals. (2010).
- 1091  
1092 65. Aronson, R. B. & Precht, W. F. White-band disease and the changing face of  
1093 Caribbean coral reefs. in *The ecology and etiology of newly emerging marine diseases*  
1094 25–38 (Springer, 2001).
- 1095  
1096 66. Casas, V. *et al.* Widespread association of a Rickettsiales-like bacterium with  
1097 reef-building corals. *Environ. Microbiol.* **6**, 1137–1148 (2004).

- 1098  
1099 67. Gignoux-Wolfsohn, S., Marks, C. J. & Vollmer, S. V. White Band Disease  
1100 transmission in the threatened coral, *Acropora cervicornis*. *Sci. Rep.* **2**, 1–3 (2012).  
1101  
1102 68. Miller, M. W., Lohr, K. E., Cameron, C. M., Williams, D. E. & Peters, E. C.  
1103 Disease dynamics and potential mitigation among restored and wild staghorn coral,  
1104 *Acropora cervicornis*. *PeerJ* **2**, e541 (2014).  
1105  
1106 69. Wan, S. J. *et al.* IL-1R and MyD88 Contribute to the Absence of a Bacterial  
1107 Microbiome on the Healthy Murine Cornea. *Front. Microbiol.* **9**, 1117 (2018).  
1108  
1109 70. Gerardo, N. M., Hoang, K. L. & Stoy, K. S. Evolution of animal immunity in the  
1110 light of beneficial symbioses. *Philos. Trans. R. Soc. Lond. B. Biol. Sci.* **375**, 20190601  
1111 (2020).  
1112  
1113 71. McFall-Ngai, M. Care for the community. *Nature* **445**, 153–153 (2007).  
1114  
1115 72. Moreira, L. A. *et al.* A Wolbachia symbiont in *Aedes aegypti* limits infection with  
1116 dengue, Chikungunya, and Plasmodium. *Cell* **139**, 1268–1278 (2009).  
1117  
1118 73. Lee, K. H. & Ruby, E. G. Effect of the Squid Host on the Abundance and  
1119 Distribution of Symbiotic *Vibrio fischeri* in Nature. *Appl. Environ. Microbiol.* **60**, 1565–  
1120 1571 (1994).  
1121  
1122 74. Visick, K. L., Foster, J., Doino, J., McFall-Ngai, M. & Ruby, E. G. *Vibrio fischeri*  
1123 lux genes play an important role in colonization and development of the host light organ.  
1124 *J. Bacteriol.* **182**, 4578–4586 (2000).  
1125  
1126 75. Broderick, N. A. Friend, foe or food? Recognition and the role of antimicrobial  
1127 peptides in gut immunity and *Drosophila*–microbe interactions. *Philos. Trans. R. Soc. B  
1128 Biol. Sci.* **371**, (2016).  
1129  
1130 76. Kwong, W. K., Engel, P., Koch, H. & Moran, N. A. Genomics and host  
1131 specialization of honey bee and bumble bee gut symbionts. *Proc. Natl. Acad. Sci.* **111**,  
1132 11509–11514 (2014).  
1133  
1134 77. Hillman, K. & Goodrich-Blair, H. Are you my symbiont? Microbial polymorphic  
1135 toxins and antimicrobial compounds as honest signals of beneficial symbiotic defensive  
1136 traits. *Curr. Opin. Microbiol.* **31**, 184–190 (2016).  
1137  
1138 78. Fuess, L. E. *et al.* Immune Gene Expression Covaries with Gut Microbiome  
1139 Composition in Stickleback. *mBio* **12**, e00145-21 (2021).  
1140  
1141 79. Davies, C. S. *et al.* Immunogenetic variation shapes the gut microbiome in a  
1142 natural vertebrate population. *Microbiome* **10**, 41 (2022).  
1143

- 1144 80. Evans, J. D. *et al.* Immune pathways and defence mechanisms in honey bees *Apis*  
1145 *mellifera*. *INSECT Mol. Biol.* **15**, 645–656 (2006).
- 1146
- 1147 81. Nyholm, S. V. & Graf, J. Knowing your friends: invertebrate innate immunity  
1148 fosters beneficial bacterial symbioses. *Nat. Rev. Microbiol.* **10**, 815–827 (2012).
- 1149
- 1150